Extraction of Silica and Iron Oxide from Municipal Solid Waste Incineration Ash and Biomass-fired Power Plant and It's Application in the Production of Magnetic Mesoporous Silica for Tetracycline Adsorption

Phan Thi Hong Hanh

A Thesis submitted in Fulfillment of the Requirement for the Degree of Master of Science in Environmental Management Prince of Songkla University 2023

Extraction of Silica and Iron Oxide from Municipal Solid Waste Incineration Ash and Biomass-fired Power Plant and It's Application in the Production of Magnetic Mesoporous Silica for Tetracycline Adsorption

Phan Thi Hong Hanh

A Thesis submitted in Fulfillment of the Requirement for the Degree of Master of Science in Environmental Management Prince of Songkla University 2023

Thesis Title   Extraction of Silica and Iron Oxide from Municipal Solid Waste Incineration Ash and Biomass-fired Power Plant and It's Application in the Production of Magnetic Mesoporous Silica for Tetracycline Adsorption

Author   Miss Phan Thi Hong Hanh

Major Program   Environmental Management

Major Advisor

....
(Assoc. Prof. Dr. Khamphe Phoungthong)

Examining Committee :

......................................Chairperson
(Asst. Prof. Dr. Montri Luengchavanon)

....Committee
(Assoc. Prof. Dr. Patiparn Punyapalakul)

....Committee
(Dr. Chomsri Choochuay)

....Committee
(Assoc. Prof. Dr. Khamphe Phoungthong)

       The Graduate School, Prince of Songkla University, has approved this thesis as fulfillment of the requirements for the Degree of Master of Science in Environmental Management.

....
(Asst. Prof. Dr. Thakerng Wongsirichot)
Acting Dean of Graduate School

This is to certify that the work here submitted is the result of the candidate's own investigations. Due acknowledgement has been made of any assistance received.

....Signature
(Assoc. Prof. Dr. Khamphe Phoungthong)
Major Advisor

....Signature
(Phan Thi Hong Hanh)
Candidate

I hereby certify that this work has not been accepted in substance for any degree, and is not being currently submitted in candidature for any degree.

......................................Signature
(Phan Thi Hong Hanh)
Candidate

Thesis Title   Extraction of Silica and Iron Oxide from Municipal Solid Waste Incineration Ash and Biomass-fired Power Plant and It's Application in the Production of Magnetic Mesoporous Silica for Tetracycline Adsorption

Author   Miss Phan Thi Hong Hanh

Major Program Environmental Management

Academic Year 2022

Abstract

Municipal solid waste incinerator and biomass power plant byproducts, namely bottom ash (BA) and fly ash (FA), are rich in silica and represent a potential source for the synthesis of silica-based materials. This study investigated the optimal conditions for alkaline fusion to extract silica from BA and FA, resulting in a supernatant solution that served as the source of silica for Magnetic mesoporous silica synthesis. To separate Fe_2O_3 from the ash, a low-temperature hydrothermal reaction was conducted using acid leaching, followed by efficient separation and extraction with methyl alcohol. Before experimentation, the mineralogical composition of the ashes was determined using X-ray fluorescence. Fourier transform-infrared (FTIR), X-ray diffraction (XRD) pattern, and scanning electron microscopy (SEM) were utilized to analyze the extracted silica and iron oxide from the ashes. Sequential extraction under these conditions yielded 71% extraction efficiency and 81% silica purification. However, the efficiency and purity of iron oxide separation are both relatively low. Subsequently, the silica and magnetic ash derived from the bottom ash were used to synthesize magnetic mesoporous silica (MMS) with a high adsorption capacity TC of 276.74 mg/g. FTIR, XRD, and SEM were also employed to characterize the MMS. Optimal conditions for overnight incubation at 60 °C and a pH of 6-8 were determined. The Langmuir isotherm and pseudo-second-order kinetic models were the optimal fitting models based on isotherm and kinetic equations. The adsorption process was identified as physisorption and spontaneous, as evidenced by the low entropy changes ($\Delta S°$), negative enthalpy changes ($\Delta H°$) of -15.94 kJ/mol, and negative Gibbs free-energy changes ($\Delta G°$).

Keywords: bottom ash, fly ash, municipal solid waste incineration, biomass power plant, magnetic mesoporous silica, adsorption tetracycline.

Acknowledgement

This thesis project has been the greatest journey for me to improve myself on being a researcher as well as a person. All the accomplishments in this work could only happen thanks to the accumulated efforts of many people.

I want to start by sincerely thanking my supervisor, Assoc. Prof. Dr. Khamphe Phoungthong. He has provided me with a great deal of knowledge, insight, and direction over the several years I spent working on my thesis. This project was made possible by his motivation, support, and constant assistance. I would especially want to thank Dr. Thitipone Suwunwong and Assoc. Prof. Dr. Suchada Chantrapromma for serving as my co-advisors in both academic and personal matters. I really appreciate everyone who gave of their time and ideas to inspire my research.

In addition, I would like to thank Scientific and Technological Instruments Center (STIC), Mae Fah Luang University, and staffs of institutes, for laboratory facilities and supporting the analysis and testing of the samples.

Next, I give my utmost gratitude to all members in our lab, thank you for helping me throughout the last 1 year and a half. Most importantly, I could not possibly go through with this project has it not been for the help of my dears support team: Pimchanok Patho, Narumon Phonrung, Sukunnika Sorasaeng, Sutthida Boonsamran, Suchanya Rongdat. The ups and downs of this thesis was less overwhelming because of them.

I would appreciate to thanks Thailand Science Research and Innovation (TSRI), grant number 652A01012 for its generous financial support.

Finally, this thesis is dedicated to my parents, my brother, my sister, and my niece, my aunt, for being tolerant of my arduous working schedules and still supportive of my decision for the last 1 year. I always admire your generosity and supporting me at all times.

Phan Thi Hong Hanh

Contents

Lists of Tables

List of Figures

List of Abbreviation/ Symbols

BA	Bottom ash
FA	Fly ash
MSWI	Municipal Solid Waste Incineration
TC	Tetracyclines
CTAB	Hexadecyltrimethyl ammonium bromide
HCl	Hydrochloric acid
NaOH	Sodium hydroxide
HNO_3	Nitric Acid
NH_4OH	Amonium
DI	Deionized water
UV-Vis	Ultraviolet–visible spectroscopy
FTIR	Fourier transform infrared spectrometry
XRD	X-ray Diffractometer
XRF	X-ray Fluorescence
SEM	Scanning electron microscopy
EDS	X-ray spectrometer
ºC	Degree celsius
wt%	Weight %
%	Percent
M	Mol

List of Published Papers

List of Paper

Hanh, P.T.H.; Phoungthong, K.; Chantrapromma, S.; Choto, P.; Thanomsilp, C.; Siriwat, P.; Wisittipanit, N.; Suwunwong, T. Adsorption of Tetracycline by Magnetic Mesoporous Silica Derived from Bottom Ash—Biomass Power Plant. Sustainability 2023, 15, 4727. https://doi.org/10.3390/su15064727.

CHAPTER 1. INTRODUCTION

1.1 Overview

In recent decades, waste production has drastically increased worldwide due to several factors such as population growth, urbanization, economic development, and changing consumer shopping habits. This trend shows no signs of slowing down. Millions tons of waste are generated by humans every year, which is becoming a significant global concern. Municipal garbage production peaked at 2.01 billion tons in 2022 worldwide, and it was expected to grow to 3.4 billion tons by 2050 as projected by World Bank [1]. These enormous amounts of waste harm the environment in many ways, including by contaminating the oceans, taking up space in landfills, contaminating underground water reserves through leachates, degrading soil, contributing to greenhouse gas emissions from decomposition and incineration, endangering the health of wildlife, and spreading diseases. As a result, modern society has significant issues in managing municipal solid waste (MSW) in a sustainable and environmentally friendly way. Landfills, the most popular method of disposal, are facing a number of challenges including a lack of dumping space close to cities, environmental degradation, odor emissions, and the release of greenhouse gases like methane [2], [3].

In a while, stricter rules were published to regulate the dumping site and the land filing procedure. In order to manage garbage more sustainably, incineration seems to be a better solution and has already been embraced by several nations. By using high-pressure steam, this technique may efficiently reduce solid waste by 90% in volume and 70% in weight [4] and it can also recover a quantity of energy [5].

However, in terms, byproducts from complete or incomplete combustion are also waste, called bottom ash (BA) and fly ash (FA) [6], which are generally hazardous in nature. The most typical way to handle these ashes is to dump them. Nevertheless, leachable heavy metals, chloride levels, and hazardous organic pollutants are present in FA and air pollution control (APC) lime. Landfilling is expensive and still poses a danger of environmental damage because it necessitates extensive pre-treatment to safeguard the dumping location. Thus, new techniques should be created to make use of these leftovers and benefit from them. The chemical analysis reveals that the major element composition of BA and FA contains a large amount of silica (60-70%), alumina (16-20%), and trace amounts of transition metals [7]. In recent years, many studies have been made to minizine the environmental impacts of ash as well as to recycle them effectively. It is mainly applied to building materials [8], ceramics [9], concrete [10], and soil amendment and fertilization [10], [11]. One of the potential elements present in this solid waste is silica which has wide applications such as water purification, adsorption, bio-sensing, catalysis, bone tissue engineering, gene and peptide delivery, tissue glue, and wound healing [12]. And others elements that have a high value are transition metals such as iron, alumina. Therefore, many studies investigated the synthesis of silica and metals have been reported [13],[14],[15]. However, these previous studies only focused on using coal BA and FA and were not concerned with separating valuable metals from slag.

In Thailand and Vietnam, which are developing countries is located in the South East Asia, many incinerators have been built for disposing of waste and also

for generating electric power [6]. Large quantities of BA and FA were insufficient technical expertise and equipment for proper treatment and disposal facilities. In addition, limited availability of appropriate applications for biomass ash, such as fertilizer production, road construction, or landfill engineering. Overall, both Thailand and Vietnam face significant challenges in managing and reusing BA and FA from MSW and Biomass Power Plants. Addressing these challenges will require a concerted effort from policymakers, investors, and local communities to promote sustainable waste management practices and explore new and innovative uses for these residues.

Nowadays, infectious disorders in both humans and animals can be effectively treated using antibiotics. Moreover, antibiotics can be utilized as preventative care and are increasingly being employed as growth boosters in agriculture and animal husbandry [16]. While, tetracycline (TC) is one of the most antibiotic popular use in the world. However, the overuse of TC leads to their enter into water environments via microbes, medical and agricultural drugs, and sewage treatment plants. This results in high residual levels of TC in the water, therefore, it is essential for removing them from water. Several methods are currently employed to remove TC from the environment, including biodegradation, electrochemical oxidation, the Fenton reaction, and adsorption. Adsorption is the process of ions and molecules physically adhering or bonding to the surface of another molecule [17]. However, this method often requires a large surface area and prolonged reaction time, which can result in the production of toxic by-products [18]. Magnetic mesoporous silica (MMS), as recently garnered increasing attention from researchers as a new adsorbent and has found extensive use in the control of environmental pollution.

This study investigated a novel approach that has the potential to extract valuable elements from incineration residues and produce the new useful material. The BA and FA from MSWI and biomass power plant effectively and economically will utilize for purely silica extraction and metal will be established. In addition, the result production will be applied to prepare MMS for adsorption TC from aqueous solution. Finally, analyze the economic advantage by comparing the cost of extracting SiO2 from these wastes to the price of the commercial product.

1.2 Objective

1. To study the physical and chemical characteristics of BA and FA from MSWI plant, and rubber biomass power plant in the southern, Thailand. And then establish the optimal conditions for synthesis of silica and iron oxides from the ashes.

2. Evaluate the economic assessment pertaining to the recycling of (BA) and (FA) waste materials for the extraction of silicon dioxide (SiO_2).

3. Synthesis MMS derives BA-biomass power plant for adsorption TC.

1.3 Outcome

This study aims to develop feasible methods to utilize MSWI ashes and biomass power plant residues in making the new materials are SiO_2, Fe_2O_3, and MMS for adsorption TC.

CHAPTER 2. LITERATURE REVIEW

2.1 Municipal Solid Waste Incineration and Biomass

The world's MSW production has significantly increased due to the rapid expansion of industry and urbanization, along with population growth, especially in large cities. The enormous amounts of waste can cause adverse effects on the environment through various means, including by polluting oceans, taking up space in landfills, contaminating underground water reserves via leachates, affecting soil quality, contributing to greenhouse emissions from decomposition and incineration, endangering the health of wildlife, and spreading diseases [19]. MSW is consists of various categories of materials. These include biogenic materials such as food waste, grass clippings, leaves, wood, paper, cardboard, and leather products. MSW also contains non-biomass combustible materials such as synthetic materials made from petroleum and plastics, as well as noncombustible materials like glass and metals. As a result, the management of MSW in a sustainable and environmentally friendly manner poses significant difficulties for modern society.

The strategies for disposing of MSW are diverse because of numerous factors including regional waste management regulations, financial constraints, collecting infrastructure, etc. The management of global waste and disposal options are shown in Figure 2.1. Open dumps are a frequent practice where one-third of the world's trash is dumped. The waste in the open ends up contaminating the environment and sanitary conditions of adjoining areas. A further third (36.7%) of the garbage is disposed of in various landfill types, such as controlled landfills, unidentified landfills, and regulated landfills. The remaining portion of the garbage is managed by more eco-friendly means, such as recycling (13.5%), composting (5.5%), and incineration (11%) [1].
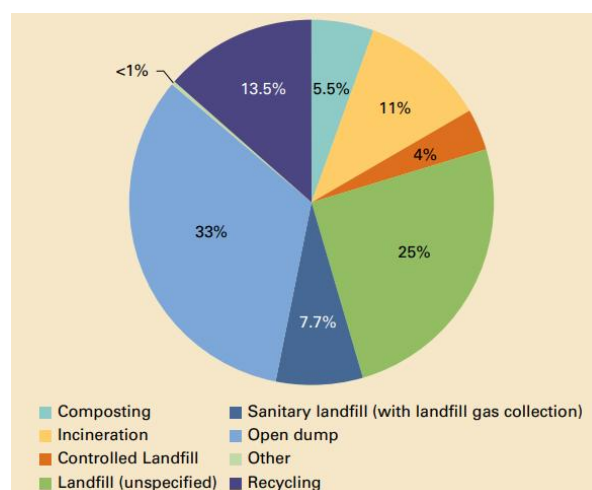

Figure 2. 1. Global Waste Treatment and Disposal [1]

Biomass, which is a renewable organic material, remains a significant source of fuel for cooking and heating in many countries, particularly in developing

nations. The use of biomass as a fuel for transportation and electricity generation is also on the rise in several developed countries, as it offers a means of reducing carbon dioxide emissions that result from the use of fossil fuels. In 2021, biomass accounted for approximately 5% of total primary energy use and provided nearly 5 quadrillion British thermal units (Btu) in the United States [20]. According to Asia-Euro Policy Dialogue (AEPD) in 2015, Thailand established a goal to increase renewable energy by 30 % by 2036, with biomass power plants being a key target with a capacity of 5,570 MW. As a result, more very small power plants, and power plants have been built in recent years [21]. And until now, Thailand has 178 biomass power plants, too [22]. Moreover, biomass fuel combustion has been seen as carbon-neutral, it could significantly contribute to the development of a clean environment [23]. Plants may capture a quantity of CO_2 that is emitted into the atmosphere during combustion through photosynthesis. Based on life-cycle analysis, there has not been a net increase in greenhouse gas emissions [24].

Today, incineration is a viable alternative to landfilling as a suitable treatment for the significant amount of MSW generated. Several countries, including developing nations, have been rapidly constructing incineration facilities in recent years [15]. By reducing the volume and weight of solid waste by approximately 90% and 70%, respectively [25], but it also generates energy and heat that could be utilized for other applications.
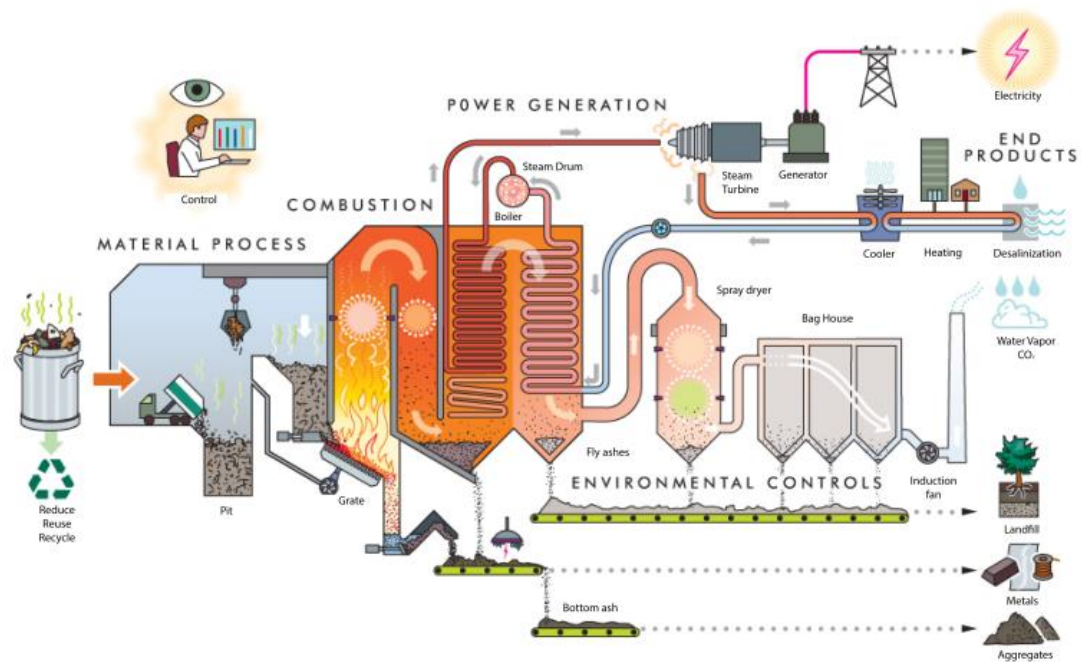

Figure 2. 2. Diagram of a waste-to-energy facility showing the incineration of MSW [26]

2.2 MSWI and Biomass Power Plant residues

However, the biggest concern of MSWI and biomass power plant, still produces a relatively large amount of solid residual materials. More than 80 % of the overall incineration ashes are accounted of the byproduct BA, which is a significant

byproduct made up of incombustible and unburned elements from the incineration process [19]. FA is the name given to the small particles that are extracted from flue gases accounted around 3%. Compared to BA, these ashes are highly polluted with potentially hazardous substances and soluble anions.

Due to various distinctions in a nation's lifestyle and garbage recycling systems, the composition of MSW varies over time and from different countries; the ash content will also vary. In general, the chemical and physical characterization of ash will be decided by the raw MSW composition, operational circumstances, incinerator type, and air pollution control system design. The chemical analysis reveals that the major element composition of BA and FA are Si, Al, Fe, Mg, Ca, K, Na and Cl, which mainly contains SiO_2, CaO, Al_2O_3, Cl_2O, Na_2O, Fe_2O_3 [27]. The most frequently metals in MSWI ash are Cr, Cu, Hg, Ni, Cd, Zn, and Pb, with Zn and Pb typically being present in the highest concentrations. Without proper treatment, these metals can damage the ecosystem and cause leaching issues. Due to metal vaporization during combustion and the process of metal adsorption on the surface of FA particles, Zn, Pb, As, Sb, Cd, and Hg concentrations in FA are typically higher than in BA [28], whereas Cu, Cr, and Ni have similar concentrations in the two ashes fractions [27]. Nowadays, numerous studies about the treatment and use of incineration residues from the last two decades have been known. In general, three treatment methods have been introduced and may be divided as follows in order to utilize waste and reduce environmental effect: 1) separation, 2) solidification/stabilization, 3) thermal method. Different treatment approaches have different mechanisms and costs, and each has advantages as well as disadvantages, as shown in Table 2.1.

Table 2. 1. Treatment methods of residues [29].

Category	Methods	Benefits	Drawbacks
Separation	Water washing	Simple Degradation of high dioxins Removing high soluble salts	Leaching process of heavy metals increased by subsequent contamination.
	Wet grinding	Simple No extra chemicals	Secondary pollution
	Electrodialysis	Efficient removal of heavy metals	Demanding in terms of technicality Expensive By-product
Solidification/	Chemical	No additional pollution	Incapable of decomposing

Stabilization	stabilization	generated	organic pollutants
	Carbonation	Utilization of CO_2 from stack gases Reducing off-gas emission Carbon sequestration	Slow process
	Cement stabilization	Stabilizing heavy metals Low cost Low technical requirement	Incapable of decomposing organic pollutants
Thermal treatment	Vitrification Melting Sintering	Significant elimination rates of chlorine and organic matter	Substantial energy consumption Significant expense Generates low-volatility oxides or alumina silicates

As a result, numerous studies have looked into how to recycle and reuse them in a variety of sectors, including agricultural, geotechnical applications, construction materials, and other uses. Table 2.2 shows the various ways that MSWI ashes and biomass power plant residues are applied in several countries [2], [30], [31].

Table 2. 2. BA and FA are widely used in many countries [2], [30], [31].

Continent	Nation	Application of ashes
Europe	United Kingdom Sweden Netherlands Italy German Denmark Belgium Poland Spain Czech Republic France	Building roads, structural foundations Constructing roads, to cap landfills Building material Constructing roads using cement Base layer of roads Subbase layer Construction material Road construction Constructing embankments, road subbase, using cement Soil surface Road construction Landfill construction

Asia	China Japan	Road construction Cement clinker

But, with the both of strategic asset and towards to a sustainable use of resources, we need study about recovering, synthesis useful materials from the ashes.

2.3 Extraction valuable elements from MSWI and Biomass residues

As the main components of MSWI ashes consist with large amount of SiO_2, therefore, it is kind of silica source with the cheap price. In general, it is possible to used residues from incineration and combustion plants to produce silica materials. Some studies have been demonstrated successful conversion of this residue to Zeolite by using alkali solution [32]. The extraction of of SiO_2 from MSWI ash synthesis of zeolite material have been also achieved [33]. Additionally, in the first time in 2007, the successful synthesis of MCM-41, SBA-15, and SBA-16 mesoporous silica has been reported [34], as well as prepared mesoporous silica through sol-gel method from municipal solid incineration bottom ash [15], and industrial ash [35]. Furthermore, silica nanoparticles were synthesized from sugar industry bottom ash [36], and paper industry fly ash [37] with alkaline extraction method.

It is economically feasible to recover some of the trace transition metals due to their present concentrations [38]. Iron is reflected to be one of the structurally essential industries shaping the economy of a country. And based on the existing literature review, municipal solid waste BA contains a significant amount of iron in the range 7 - 15% [39]. It can be a valuable resource, can serve as a supplemental source of iron supply, if recovered profitably. Recovering and extracting these metals appear to be environmental and economic option compared to disposing the ash in a landfill following the immobilization process. Various methods using different leaching reagents have been investigated, such as: water leaching [40], acid leaching [25,26], alkaline leaching [43], bioleaching [28]. Typically, these approaches involve extracting the metals through leaching using acid, alkaline or other agents, followed by filtration and chemical precipitation to recover the dissolved metals in the solution. Until now, have some investigations reported about the extraction iron from ash such as: a high iron recovery of 42.4% from steel slag have been demonstrated by magnetic separation [45], metals oxides from coal bottom ash waste by carbon reduction [46], metal oxides successfully extracted from the coal bottom ash by acid leaching [47]. However, many previous studies didn't separate the metals from ash, and used the material from coal ash. And, the general incinerated ash slag has rarely been used for extraction of silica and metals, most studies on its use as a civil-engineering building materials, despite its high silica and metals content.

2.4 Antibiotic (tetracycline) contaminant and method for treatment

Antibiotics are synthetic or semisynthetic drugs by a natural way, which have been widely used in human medicine and livestock animals for prophylactic, therapeutic, and growth promoting purposes [48]. Cycon et al., 2019, analyzed the situation in 75 countries and found that there was a 65% increase in

antibiotics usage. They predict that by 2030, the consumption of antibiotics will be 200% higher than it was in 2015 [49]. The widespread use of antibiotics has become a serious problem as it may pose many significant threats to human health, such as antimicrobial resistance, allergic reactions and gastrointestinal disturbance [50]. TC is a widely used and inexpensive antibiotic that is effective against a broad spectrum of bacterial in both human and veterinary medicine as well as in agriculture [51]. It is frequently utilized as an animal growth promoter [52]. As one of the most massively produced and utilized antibiotic families [53]. TC is highly soluble in water and has been found in various environmental settings , including surface water (ranging from 5.4 to 8.1 ng/L) [54], ground water (greater than 100 ng/L) [55], MSW, and soil (ranging from 86.2 to 198.7 µg/kg) [56]. Moreover, it can be easily transferred to other environments via aqueous matrixes [57]. Due to its naphthol ring structure, TC is difficult to degrade and thus can persist in the environment [58]. This is compounded by the fact that a significant portion of the administered drug is excreted by humans and animals and can end up in domestic wastewater and pits where sludges are deposited [49]. However, conventional water treatment and biodegradation methods have proven to be ineffective in removing TC from aqueous solution [59][60]. As a results, there has been a growing interest in developing efficient and secure techniques for TC removal. Methods for TC removal include oxidation [61], photo electrocatalytic [62], degradation [63], membrane processing [64], adsorption [65], permeation [66], flocculation [66], ozonation oxidation [66]. Among these, adsorption emerged as a promising method due to its ease for operation, low costs, and significant removal efficiency at extremely low TC content in wastewater and water [67]. Particularly, no generation of toxicity of intermediates and by-products during adsorption makes it a safer alternative to other methods [68].

Until now, various materials such as graphene oxide [69], activated carbon [70], kaolinite [71], single-walled carbon nanotubes, and multi-walled carbon nanotubes [60] have been studies for their ability to adsorb and remove TC. Carbon nanotubes and graphene, in particular, have been found to be highly effective due to their graphite structure [72]. However, cost associated with manufacturing, disposing, and regenerating these materials are prohibitively high, making them unsuitable for large-scale TC adsorption applications. Therefore, there is significant need for the development of low-cost, easy-to-use, and highly selective devices that are both efficient and affordable.

MMS had the characteristics of mesoporous silica (small particles size,large surface area, big pore size and volume) and magnetic particles could be rapidly separated by the application of an external magnet [40], so it can be used as an adsorbent. Therefore, using it for removing toxic elements and compounds from contaminated water is emerging. However, the adsorbent should have a consistent pore arrangement, homogeneous particle size, and a small pore size to increase adsorption efficiency. Until now, have some report investigated this problem for example, mesoporous silica materials for the elimination of heavy metals (Pb^{2+}, Cu^{2+}, Cd^{2+}, and Cr^{2+}) from aqueous solutions with support in surfactant solution Hexadecyltrimethyl ammonium bromide (CTAB) [35], silica nano particles were achieved with uniform and small particle size of 20–30 nm with presence of 3 wt% CTAB [73]. So, CTAB have a great impact on morphology, which can help achieve

uniform size of the mesoporous structure for the nanoparticles. And in our study, CTAB are considered as a template of adsorbent.

In this study, BA and FA from MSWI and biomass power plant, will be used as the materials for synthesis silica and iron oxides via alkali treatment and acid leaching, respectively. Furthermore, prepare magnetic mesoporous silica from the above results for adsorption antibiotic groups: tetracyclines (TC).

CHAPTER 3. MATERIAL AND METHOD

3.1 Material

The BA and FA were collected from Phuket Municipal Waste Incineration Plant, and the Rubber Biomass Power Plant of Gulf Yala Company in Southern, Thailand.

Phuket's Municipal Waste Power Plant (Phuket waste to energy plant) is a 14 kW biopower project, which located in Saphan Hin, Phuket, Thailand. The factory got commissioned in November 2012. The incinerator has full capacity to burn 900 tons of garbage per day and produce 14,000 kW power [74].

The Yala biomass generation plant, a facility constructed by Gulf Yala Green Co., Ltd., which began operating in November 2008. The facility is capable of producing a maximum output power of 20,000 kW by incineration of rubber wood waste [75].

3.2 Instruments

- X-ray Diffractometer (XRD) - X'Pert Pro MPD, Malvern Pananalytical, Bruker AXS Advance, United Kingdom.

- X-ray Fluorescence (XRF) - S2175 Ranger, Bruker, Burladingen, Germany.

- Fourier transform infrared spectrometry (FT-IR) - Perkin Elmer Model Spectrum GX - Thermo Fisher, Nicolet iS5, USA.

- Scanning electron microscopy (SEM) - Apreo, FEI, South Moravian Region, Czech Republic.

- X-ray spectrometer (EDS) - (X-Max80, Oxford, UK).

- Ultraviolet–visible spectroscopy -C-7200 PEAK Instruments Inc, USA.

- Oven, UF 110, Memmert GmbH + Co. KG, Schwabach, Germany.

- Analytical balance, ML204 /01, Mettler Toledo, Switzerland.

- Hotplate stirrers, IKA C-MAG HS2, Staufen, German.

- pH meter, HI 2211, Hana Instrument, US.

3.3 Chemical and Reagents

Table 3. 1. List chemicals, reagents and supplier

No.	Name	Grade	Supplier/ Source
1	Sodium Hydroxide (NaOH)	Analytical	Loba Chemie PVT.LTD, India
2	Deionized water	Analytical	School of Science, Mae Fah Luang University, Thailand
3	Hydrochloric Acid (HCl) 37%	Analytical	Qrec, Newzealand
4	Nitric Acid (HNO$_3$)	Analytical	Qrec, Newzealand
5	Amonium (NH$_4$OH)	Analytical	Loba Chemie PVT.LTD, India
6	Hexadecyltrimethyl ammonium bromide (CTAB) $\geq$ 98%	Analytical	Sigma-Aldrich, Cibolo, TX, USA
7	Tetracycline hydrochloride, 96% (C$_{22}$H$_{25}$ClN$_2$O$_8$)	Analytical	Alfa Aesar, United Kingdom
8	Poly(vinyl alcohol)	Analytical	Sigma-Aldrich, USA
9	Ethanol 99%	Analytical	Qrec, Newzealand
10	Glycerol (C$_3$H$_8$O$_3$)	Analytical	Qrec, Newzealand.

3.4 Experimental Method

3.4.1 Prepare and analyze samples

Firstly, samples (BA from MSWI and Biomass power plant) were washed twice-three time with tap water and then was ground in a hi-speed Mill Machine (Model single-head for hi-speed) and sieved to get a particle size of under 75 μm (200-mesh sieve). After that, continue washed several times with distilled water filtered and dried at a constant temperature of 90 °C to remove moisture for 24 hours. FA from Biomass power plant were washed several times with distilled water, and then filtered and dried with the same BA samples.

The samples were stored in a closed container to protect it from moisture until use. The samples will be analyzed by the mineral and chemical by X-ray Fluorescence (XRF) spectroscopy.

3.4.2 Experimental design

Figure 3. 1 presented the schematic diagram of the procedure of the experiment of the thesis.
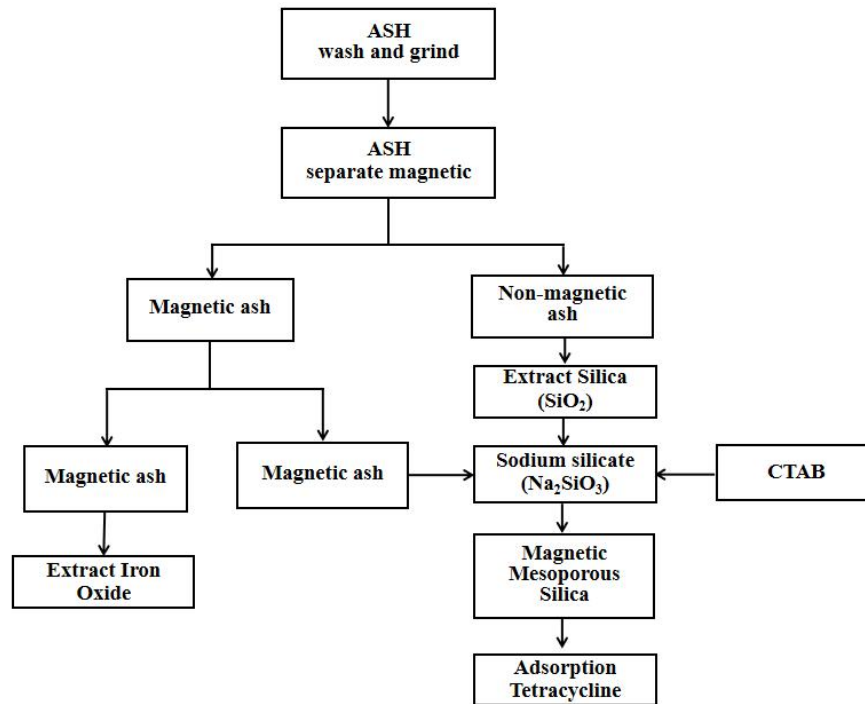

Figure 3. 1. The schematic diagram showing the procedure of the experiment

- Experiment 1: Synthesis purity Silica (SiO_2)

In this work, investigators synthesized nanosilica from BA and FA of Phuket MSWI and Yala Rubber biomass power plant by alkali dissolution and sol-gel methods according to Yadav, V.K. et al., with some modification [76].

First, put 5 g of ash into the beaker and separated the magnetic and non-magnetic ash with a magnet. Then, it was dried at 90 °C for 12 h. And non-magnetic ash will be re-fluxing with NaOH solution with different concentrations of 3M, 4M, and 5M at 90 °C for 8h, 16h, and 24h in the round bottom flask. The reacted solution will be then filtered through a membrane of 0.45 μm and collected supernatant for adjusting pH at 7 by HCl 5 M. The solution was aged at room temperature for 24h, then filtration and washed with DI water several times, and dried in the oven at 90 °C for 1 day. The solid residues will be analyzed for checking the purity and characterization of SiO_2: XRF analysis will be used for determining the content of constituents of the silica extracted, and XRD to determine the structural pattern of the produced materials; FTIR for identify the organic groups on the surface of the produced materials, as well as SEM was used to examine the surface. The experimental scheme for the extraction SiO_2 process is shown in Figure 3.2. The yield of silica will be calculated using Eq. (1) .

$$\% \text{ Yield} = \frac{\text{Dried weight of obtained silica} \times \% \text{ purify of SiO}_2}{\text{Dried weight SiO}_2 \text{ from the ash}} \times 100 \qquad (1)$$
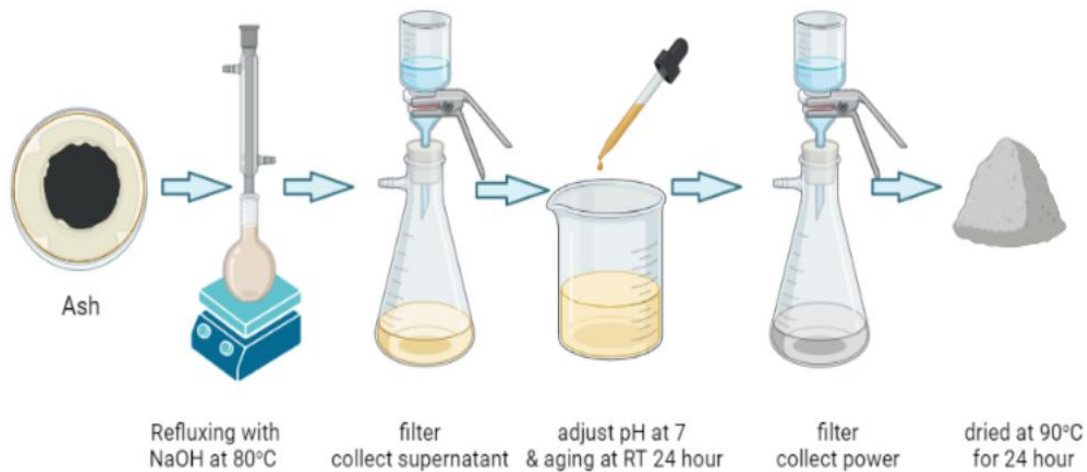

Figure 3. 2. The procedure for the SiO_2 extraction

- Experiment *2:* Synthesis of Iron Oxides (Fe_2O_3)

This study used the co-precipitation method described in the patent CN105776345A [77], with some modification that is suitable for the characteristic of the sample. By using this technique, the ash resource is fully exploited, the production process is straightforward, the cost of production is low, and the approach is appropriate for mass production. Using the method, Fe_2O_3 in ash can be effectively separated and extracted; Al_2O_3 in ash can be dissolved out by 90%-96%. Additionally, no special equipment is needed; all that is required is a low-temperature reaction. The experimental scheme for the extraction metal process is shown in Figure 3.3.

Firstly, magnetic particles were separated from the ashes by using a magnet. Then, magnetic ashes were mixed with HNO_3 5% at a solid-to-liquid ratio of 1:5 and reacted at 80 °C for 1-2 hours. Once the reaction was completed and cooled to room temperature, the resulting mixture was filtered and washed with distilled water at a solid-to-liquid ratio of 1:2. This solution contained iron nitrate and aluminum nitrate. Next, methanol was added to the mixture at a volume ratio of 12:1. An amount of NH_4NO_3 was added to the mixture in a molar ratio of 1:3 ($Al(NO_3)_3$:NH_4NO_3) and stirred for 1-2 hours. The resulting mixture was then filtered, and the aluminum nitrate powder was obtained. The powder was washed with methanol at a ratio of 1:2 (alumina:methanol), and the residue was collected on the filtrate. To obtain iron hydroxide, NH_4OH was added drop by drop to the solution until the pH > 8. Then, the supernatant was aged at room temperature for 2-3 hours, filtered, and dried at 80 °C for 24 hours to collect iron oxide. The results will be analyzed for checking the purity

and characterization of Iron Oxide and compared with the chemical analysis of the samples.
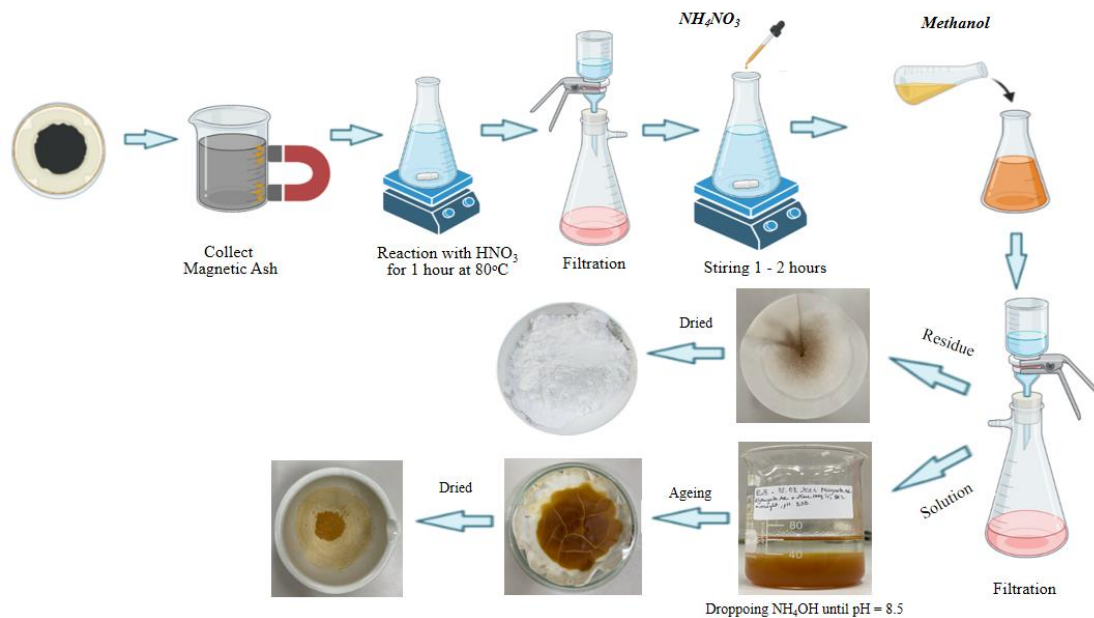

Figure 3. 3. The procedure for the metal extraction

- Experiment 3: Preparation Magnetic Mesoporous Silica for TC adsorption.

The preparation of magnetite mesoporous silica (MMS) was carried out using a method previously reported by C. Azmiyawati et al., 2020 [78], with some modifications. Magnetic and nonmagnetic ashes were separated using permanent magnets, with the magnetic ash serving as the magnetic component in MMS and nonmagnetic ash being used to extract silica. The weight ratio of magnetic and nonmagnetic ashes was 1:10.

The SiO_2 obtained from Bottom Ash – Biomass power plant were used to prepare the sodium silicate solution by dissolving SiO_2 and NaOH (4:5 w/w ratio) in 250 mL of distilled water at 80 °C for 1 day [79].

A clear solution was obtained by adding 1.2 g of hexadecyltrimethyl ammonium bromide (CTAB) to 20ml of deionized water and then mixed at 40°. This aqueous CTAB solution was then mixed with sodium silicate solution and stirred for 15 min. The resulting mixture was slowly added to the magnetic ash at a ratio of 1:20 maghemite to Na_2SiO_3 10%, while being stirred and heated to 80 °C. After stirring for 30 min, the pH of the mixture was adjusted to 11 by 5 mol/L HCl solution and stirred continuously for 6 hours. The mixture was kept in a water bath at 80 °C for 72 hours, followed by the addition of 100 mL ethanol 99.9% to precipitated product. To remove CTAB, the mixture was sonicated for 30 min at 60 °C [80], and washed with DI water multiple times, and dried at 80 °C for 24 hours. The synthesis process of magnetic mesoporous silica is demonstrated in Figure 3.4.
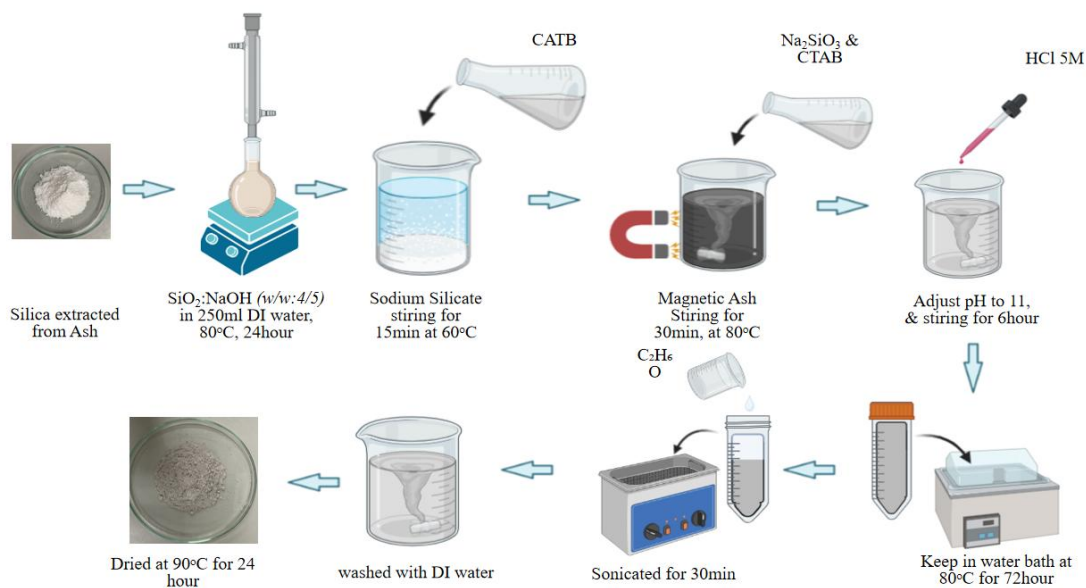
Figure 3. 4. The procedure for preparation Magnetic mesoporous silica

The mineral elements MMS were analyzing by X-ray fluorescence (XRF), (S2175 Ranger, Bruker, Burladingen, Germany). Fourier transform infrared spectroscopy FT-IR (Perkin Elmer Model Spectrum GX) was used to analyze the specific functional groups of the adsorbents by compressed samples into KBr pellets and then analyzed with a Nicole IS10 spectrometer over the wavelength ranged from 400 to 4000 cm^{-1}. X-ray diffraction (XRD) pattern (PAN analytical, X'Pert Pro MPD) was performed on a Bruker AXS Advance instrument for confirmation the structure. The surface morphology of MMS was examined by scanning electron microscopy (SEM, Apreo, FEI, South Moravian Region, Czech Republic) running by Schottky field emission at the accelerating voltage of 20 kV in high vacuum mode. The elemental mapping analysis of the sample was conducted using the energy-dispersive X-ray spectrometer (EDS)-(X-Max80, Oxford, UK).

MMS was used to adsorb TC in an aqueous solution, and the impact of adsorption time and temperature on the unit adsorption capacity and adsorption rate of TC was investigated to determine the ideal conditions. MMS (3 mg) was dispersed in a flask containing 10.0 mL TC solution with various concentrations (10–100 mg/L), pH 6–8, and fully homogenized with a vortex mixer. The suspension was incubated overnight at 25 °C, 45 °C, and 60 °C and covered with aluminum foil to protect TC from the potential photo degradation. MMS was separated from the samples through a magnet after centrifuging at 2000 rpm for 15, 30, 45, 60, and 90 min while maintaining the experiment temperature including centrifugation. The residual concentration of TC in an aqueous solution was determined by UV–vis absorbance at 357 nm, using a calibration curve built. All the experiments were replicated thrice, and the averaged results were reported. Equation (2) was used to calculate the percentage removal of TC, and Equation (3) was used to determine the adsorption capacity:

$$Removal(\%) = \frac{(C_o - C_e)}{C_o} \, x \, 100 \tag{2}$$

$$Q_e = \frac{(C_o - C_e) \, x \, V}{m} \tag{3}$$

where:
C_o is the initial concentration of TCs (mg/mL);
C_e (mg/L) is the equilibrium concentration of TC;
V is the solution volume (mL);
m is the mass of adsorbent (g).

The experimental scheme for remove TCs from aqueous by magnetic mesoporous silica is shown in Figure 3.5.
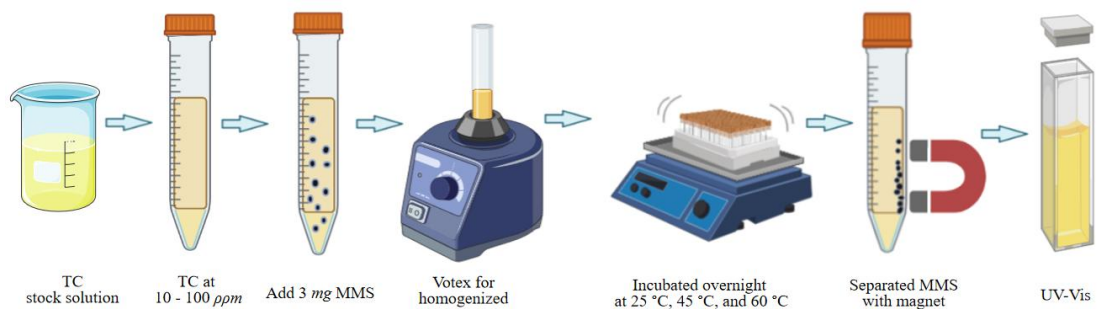
Figure 3. 5. The diagram TC adsorption on MMS from aqueous

3.5 Economic evaluation

In the economic evaluation, several assumptions will be used based on all apparatus' specification, prices for raw materials/ chemicals, electricity, and the labor cost follow Nandiyanto, A. B. D. (2018) [81] with some modifications for suitable with our research. And then calculate the price for produces 1kg SiO_2 from waste and compared to the selling the price.

In order to conduct an accurate economic analysis, certain assumptions were made to anticipate and evaluate various possibilities that could arise during the project. These assumptions include:

1. Using the USD as the currency for all analyses.

2. Assuming the prices of NaOH and silica to be 0.6 and 5 USD/kg, respectively, based on commercially available prices. The price of HCl (33%) was assumed to be 0.30 USD/L. These estimates were based on the chemical reaction mechanism.

3. And the material cost of ashes is free.

4. The process of converting ashes to silica particles takes one cycle with 16 hours to complete.

5. To simplify the utility system, the unit of utility can be simplified and converted to kWh (kilowatt hours) of electricity [82]. This allows for easy conversion into cost by multiplying with the standard minimum electricity cost, which is 0.15 USD/kWh [81].

6. The labor cost per processing cycle amounts to 8.56 USD in total [81].

The production cost was calculated according to the equation:

Production cost = (raw materials cost + labor cost + manufacturing   (4)
cost) / amount of product produced during that period.

where:

raw materials cost = quantity used × purchase price/amount of all   (4.1)

labor cost = earned income/ number of products produced   (4.2)

manufacturing cost = electricity cost × number of production hours   (4.3)

CHAPTER 4. RESULTS AND DISCUSSION

4.1 Characteristics of Ash

Figure 4.1 show the visual of the samples of BA and FA from MSWI and biomass power plant. Fresh BA has a high-water content and a faintly unpleasant smell since it needs to be cooled by water washing. The large-diameter BA is primarily composed of ceramic pieces, bricks, and metal products, while the small-diameter portion is predominantly made up of glass and ash. The composition of BA consists mainly composed of Si, Ca, Al, Fe and other elements. The higher SiO_2 and CaO ratio in BA, as compared to FA, is especially advantageous in enhancing the strength of BA. BA includes smaller heavy metals than FA, which is more ecologically friendly (Table 4.1). FA is gray or dark gray with fine particles. Because of its high porosity and capacity for adsorption, FA contains certain volatile heavy metals adsorbed on its surface [83].
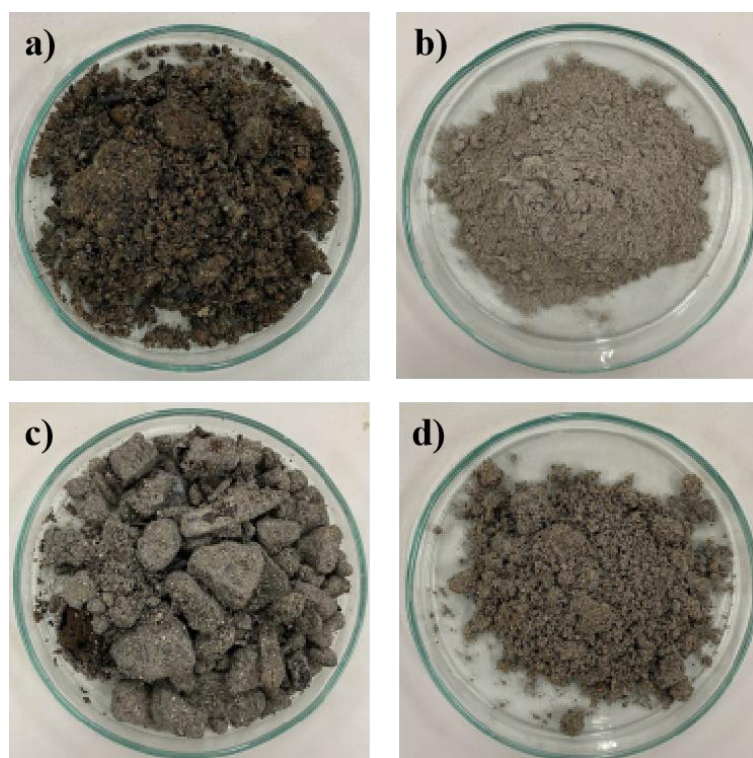
Figure 4. 1. The picture of the sample: a). BA-Biomass Power Plant; b). FA-Biomass Power Plant; c). BA-MSWI, d). FA-MSWI.

Table 4.1 lists the chemical composition of the BA and FA from MSWI and Biomass power plant were used. The chemical analysis indicated that the component consisting of SiO_2 accounted for 36.56, 55.52, 37.55 wt.% of the total content from the BA-MSWI, BA-Biomass power plant, FA-Biomass power plant, respectively. And the Fe_2O_3 content was 7.7 wt.% from BA-Biomass power plant.

The FA-MSWI samples was not extracted SiO_2 in this investigation, due to containing only a minor amount of silica.

Table 4. 1. Chemical compositions of the materials by XRF

Compound	BA-MSWI (wt. %)	FA-MSWI (wt. %)	BA-Biomass power plant (wt. %)	FA-Biomass power plant (wt. %)
Na_2O	3.23	4.04	0.09	0.11
MgO	2.72	0.58	2.35	4.37
Al_2O_3	4.65	0.45	10.67	8.55
SiO_2	36.56	1.36	55.52	37.55
P_2O_5	3.24	0.31	1.06	2.38
SO_3	2.18	3.16	0.36	4.65
Cl	2.94	24.82	0.07	0.64
Br	0.03	0.16		
CHNO	6.18	16.19	4.42	7.20
K_2O	1.61	4.65	5.92	10.19
CaO	30.44	42.64	10.48	19.67
TiO_2	0.97	0.24	0.81	0.72
Cr_2O_3	0.13	0.02	0.07	0.04
MnO	0.09	0.02	0.29	0.32
Fe_2O_3	4.15	0.41	7.70	3.32
NiO	0.01		0.01	0.01
BaO	0.18			
CuO	0.09	0.06	0.02	0.02
ZnO	0.21	0.61	0.01	0.05
Rb_2O	0.01	0.02	0.04	0.07
SrO	0.13	0.04	0.04	0.06
ZrO_2	0.05		0.06	0.06
SnO_2	0.02	0.06		
Sb_2O_3	0.01	0.03		
PbO	0.17	0.13	0.01	0.02

4.2 Synthesis SiO$_2$ from BA and FA.

The chemical content of the white powers was measured by X-ray Fluorescence Spectroscopy (XRF) was shown in the Table 4.2. The amount of SiO$_2$ up to 81.48, 75.65, 52.86 wt.% was obtained by refluxing in NaOH 4M solution, at 90 °C for 16 hours from BA-MSWI, BA-Biomass power plant, FA-Biomass power plant. Trace a number of impurities were also found such as Al$_2$O$_3$, K$_2$O, CaO, MgO, MnO$_2$, and P$_2$O$_5$.

Table 4. 2. Chemical composition of SiO$_2$ extracted from samples

Compound	BA MSWI (wt %)	BA Biomass power plant (wt %)	FA Biomass power plant (wt %)
Na$_2$O	4.43 ± 2.11	4.34 ± 2.11	7.35 ± 3.00
Al$_2$O$_3$	5.55 ± 4.46	5.56 ± 4.46	17.75 ± 11.14
SiO$_2$	81.48 ± 1.53	75.65 ± 11.4	52.86 ± 15.53
P$_2$O$_5$	0.03 ± 0.00	0.07 ± 0.08	1.02 ± 0.89
SO$_3$	0.02 ± 0.01	0.02 ± 0.00	-
Cl	0.50 ± 0.56	3.99 ± 4.41	3.63 ± 0.42
K$_2$O	0.14 ± 0.01	0.44 ± 0.33	1.34 ± 0.54
Fe$_2$O$_3$	0.16 ± 0.06	0.55 ± 0.49	0.54 ± 0.11
CuO	0.04 ± 0.01	0.03 ± 0.01	0.05 ± 0.00
ZnO	0.31 ± 0.31	0.12 ± 0.18	0.22 ± 0.28
PbO	0.25 ± 0.03	0.20 ± 0.00	0.08 ± 0.00
CaO	0.03 ± 0.00	-	0.04 ± 0.00
TiO$_2$	0.03 ±0.00	0.07 ± 0.00	0.06 ± 0.02
Cr$_2$O$_3$	0.03 ± 0.00	-	
MnO	-	-	0.06 ± 0.00
Rb$_2$O	-	0.01 ± 0.00	0.02 ± 0.00
CHNO	8.45 ± 0.18	9.03 ± 2.08	14.09 ± 0.16

The XRD patterns of the extracted SiO_2 from BA-MSWI, BA-Biomass Power Plant, and FA-Biomass Power Plant were displayed in Figure 4. 2 (a-c). The prepared powders exhibited the board peaks that appeared around $2\theta = 22°$, which indicated the presence of silica particles. The disappearance of sharp peaks in the XRD pattern of silica nano powders confirmed an amorphous nature, and did not appear in the zeolite or crystalline phase, indicating a comparatively high degree of disordered structure in silica [84].
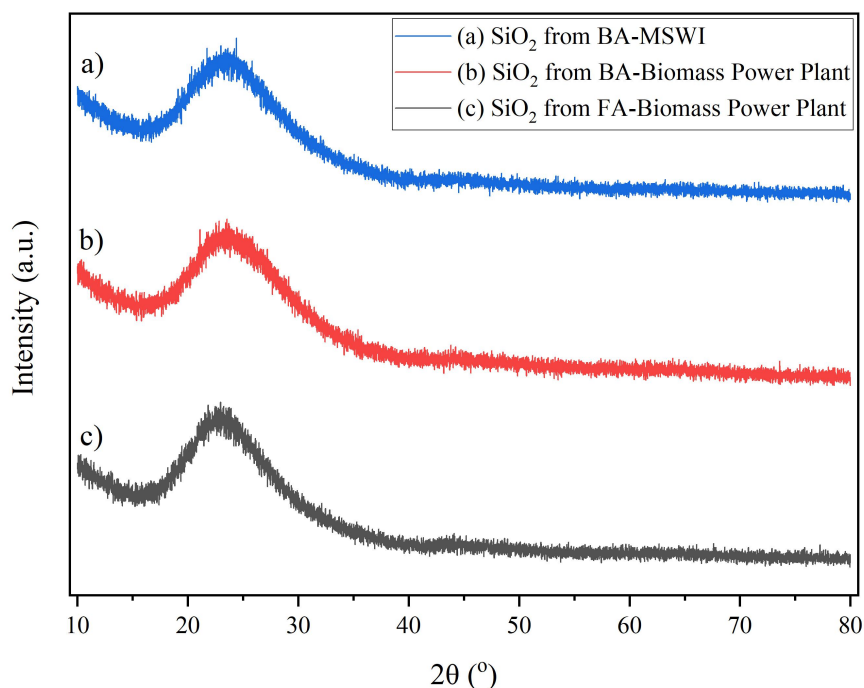
Figure 4. 2. XRD patterns of SiO_2 extracted from BA-MSWI (a); BA-Biomass Power Plant (b); FA-Biomass Power Plant (c).

The silica powders were confirmed by FT-IR examination in Fig 4.3. The broad peak from 3000 to 3700 cm^{-1} was assigned to the presence of O-H group [85]. Similarly to this, a peak matching to vibration bending may be seen at 1633 to 1644 cm^{-1}, indicating the presence of an O-H stretching bond [86]. Additionally, the strong bands at 1025, 1085, and 1097 cm^{-1} was associated to the asymmetric and symmetric Si-O-Si stretching vibration bindings [87].
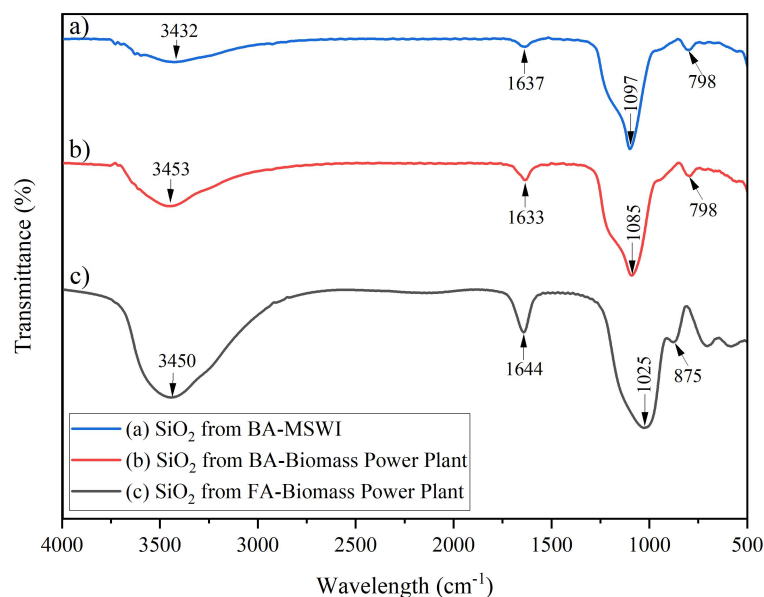
Figure 4. 3. FTIR spectra of SiO$_2$ extracted from BA-MSWI (a); BA-Biomass Power Plant (b); FA-Biomass Power Plant (c).

By using the reflux process and alkaline extraction, amorphous silica was successfully created. The surface morphology of the amorphous silica was examined using SEM pictures. As shown in Figure 4.4, the grain of the synthetic silica made from ashes has an irregular shape and a size of 9–12 nm. Amorphous silica is indicated by surfaces that are brightly colored, while pore cavities are shown by surfaces that are darkly colored [88]. The SEM picture shows that the agglomeration of spherical particles, which formed through the aggregation of fine homogeneous grains of nano size.
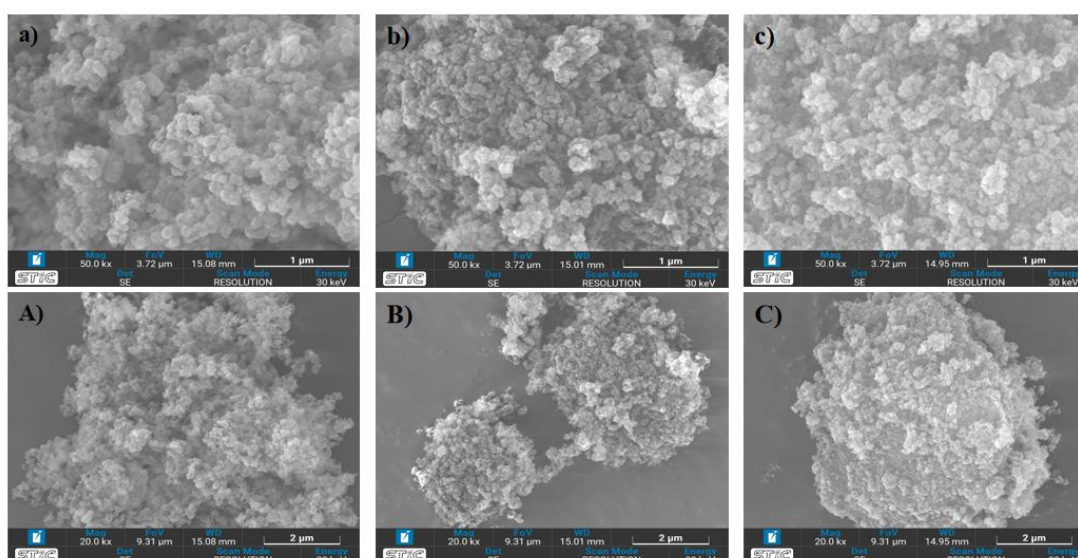

Figure 4. 4. SEM of SiO$_2$ extracted from BA-MSWI (a, A); BA-Biomass Power Plant (b, B); FA-Biomass Power Plant (c, C)-(a,b,c~Mag 50.0 kx, A,B,C~Mag 20.0 kx).

- The mechanism of Silica extraction process from Ash

BA and FA contained a silica composition of 35 to 55%, followed by alumina, ferrous and traces, and then Ca, K, P, etc. Silica is acid-insoluble and could react easily with strong hydroxides (NaOH) at 90–95 ◦C for 16 hours along with stirring by the alkali–dissolution method. The three essential processes of such a technique are extraction of silicates from the source (BA&FA), condensation, and drying to produce powdered silica. After filtering and titrating with diluted HCl (5 M) as a precipitating agent, the produced alkaline sodium silicate was precipitated. At the top of the beaker, a clear gel developed. As seen in the Reactions (1-3), the silicate was extracted from the BA & FA in the form of crude sodium silicate, which was followed by the formation of silicon hydroxides in the presence of HCl at a pH of around 7–8. At this stage, the silicon hydroxide species undergo condensation to create a silicone bond (Si-O-Si). Finally, condensation and drying were performed to produce silica. Yadav, V.K. and et al., reported a similar observation during floral-shaped nano silica production from coal FA [76].

$$SiO_2 \ (BA\&FA) + 2NaOH \rightarrow Na_2SiO_3 + H_2O \qquad (1)$$

$$Na_2SiO_3 + 2H_2O + 2HCl \rightarrow Si(OH)_4 + 2NaCl \qquad (2)$$

$$= Si - OH + = Si - OH \rightarrow = Si - O - Si + H_2O \qquad (3)$$
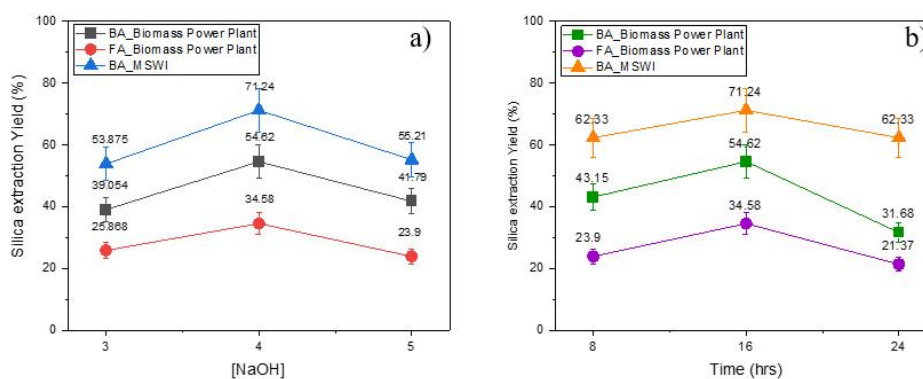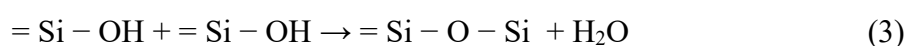
Figure 4. 5. Condition optimization for maximum silica extraction (a) effect of the molar concentration of NaOH (3-5 M), (b) effect of reaction time (8-24 hours)

The concentration of the alkaline solution and reaction time have the most effects on the amount of silica that can be extracted from the sample. Figure 4.5a shows the impact of sodium hydroxide solution's molar concentration on the extraction of silica. The figure shows that silica extraction increases as sodium hydroxide solution concentration rises up to 4M. The amount of silica is seen to decrease above this concentration, hence 4M concentration is the optimal value. Figure 4.5b shows the impact of reaction time on silica extraction. It has been

discovered that reaction time has a higher impact on silica extraction effectiveness. An increase in the extraction of silica was seen when the reaction time increased from 9 to 16 hours. Silica extraction virtually stops at 24 hours, which means that the entire amorphous silica reacts with sodium hydroxide at 16 hours.

4.3 Synthesis of Iron Oxides (Fe$_2$O$_3$)

According to the X-ray diffraction analysis (Figure 4.6) showed the obtained the iron oxide extract from BA-Biomass Power Plant and standard Fe$_2$O$_3$. The obtained fraction of iron oxide indicated a low concentration of iron oxide, making it difficult to identify the primary iron minerals.
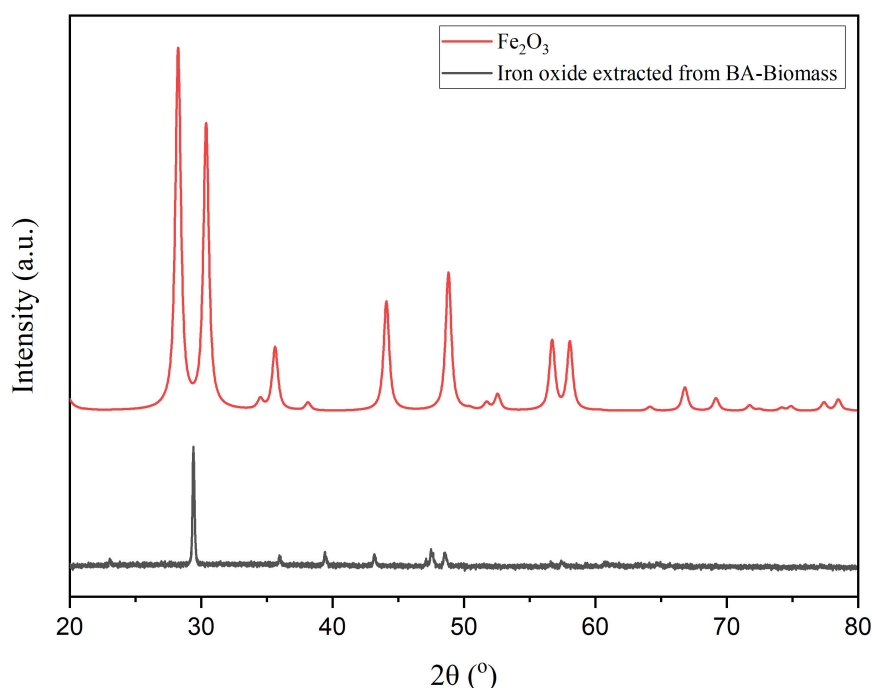

Figure 4. 6. XRD of the iron oxide extract from BA-Biomass Power Plant and standard Fe$_2$O$_3$.

The quantitative analysis of elements by XRF (Table 4.3) presented that Fe$_2$O$_3$ contained only 18.31 %. Various traces of impurities, including Al$_2$O$_3$, K$_2$O, CaO, MgO, MnO$_2$, and P$_2$O$_5$, were also discovered, and a large amount of SiO$_2$ accounted for 20.56%.

Table 4. 3. XRF of iron oxide extracted from BA - Biomass Power Plant

Compound	Conc. (%)	Compound	Conc. (%)	Compound	Conc. (%)
Na_2O	0.09	SO_3	0.24	CuO	0.08
MgO	4.29	Cl	0.21	Fe_2O_3	18.31
Al_2O_3	16.30	K_2O	0.23	ZnO	0.07
SiO_2	20.56	CaO	5.14	Y_2O_3	0.01
P_2O_5	2.68	TiO_2	0.82	ZrO_2	0.01
Cr_2O_3	0.05	Co_3O_4	1.05	PbO	0.02
As_2O_3	0.02	SrO	0.03		
MnO	1.56	NiO	0.50	CHNO	27.73
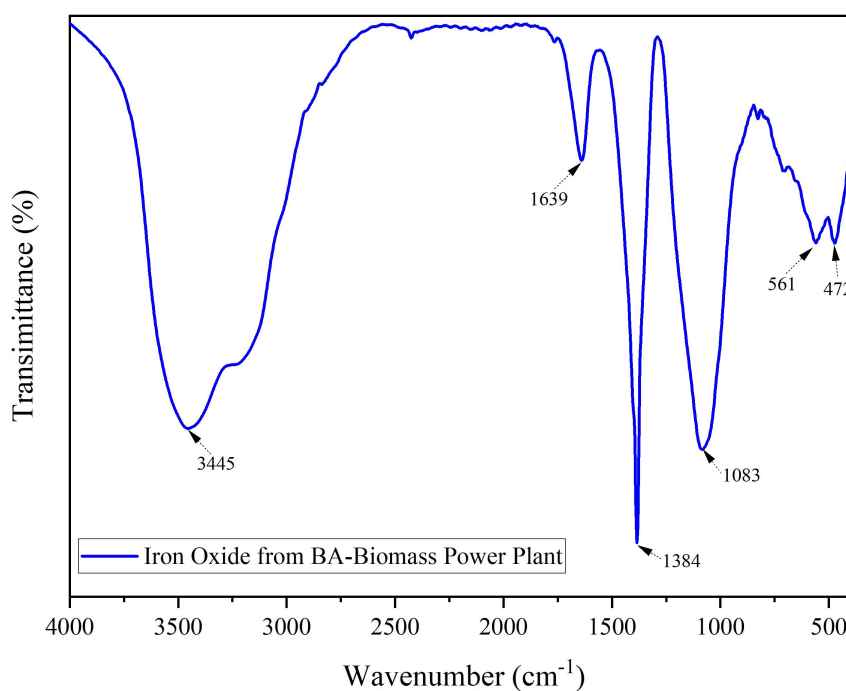
Figure 4. 7. FTIR spectra of the iron oxide from BA-Biomass Power Plant

Based on Figure 4.7, the FTIR of iron oxide extracted from BA-Biomass Power Plant were in the range of 4000 cm^{-1} to 500 cm^{-1} wave number which provides the chemical bonds and functional groups in the products. The large broad band at 3445 cm^{-1} and 1739 cm^{-1} was ascribed to the O-H stretching vibration in O-H groups. The characteristic absorption bands of the sample at 561 cm^{-1} and 472 cm^{-1} referred to the stretching vibrations of Fe–O bonds [89]. The sharp peaks at 1384 cm^{-1} and 1082 cm^{-1} were maybe indicated of the Si-O bonds, which could be impurities of the products.

The morphology analysis in Figure 4.8 with different magnifications, shows that iron oxide extracted from BA-Biomass Power Plant is presented in an irregular flocculent distribution with a loose structure and rough surface. Meanwhile, based on XRF monitoring data in Table 4.3, it is obvious that the red power product consists of O, Ca, Si, Al, … and other trace elements product. However, the content of Fe_2O_3 is higher than that of Pb, Cu, Zn, and Ni.
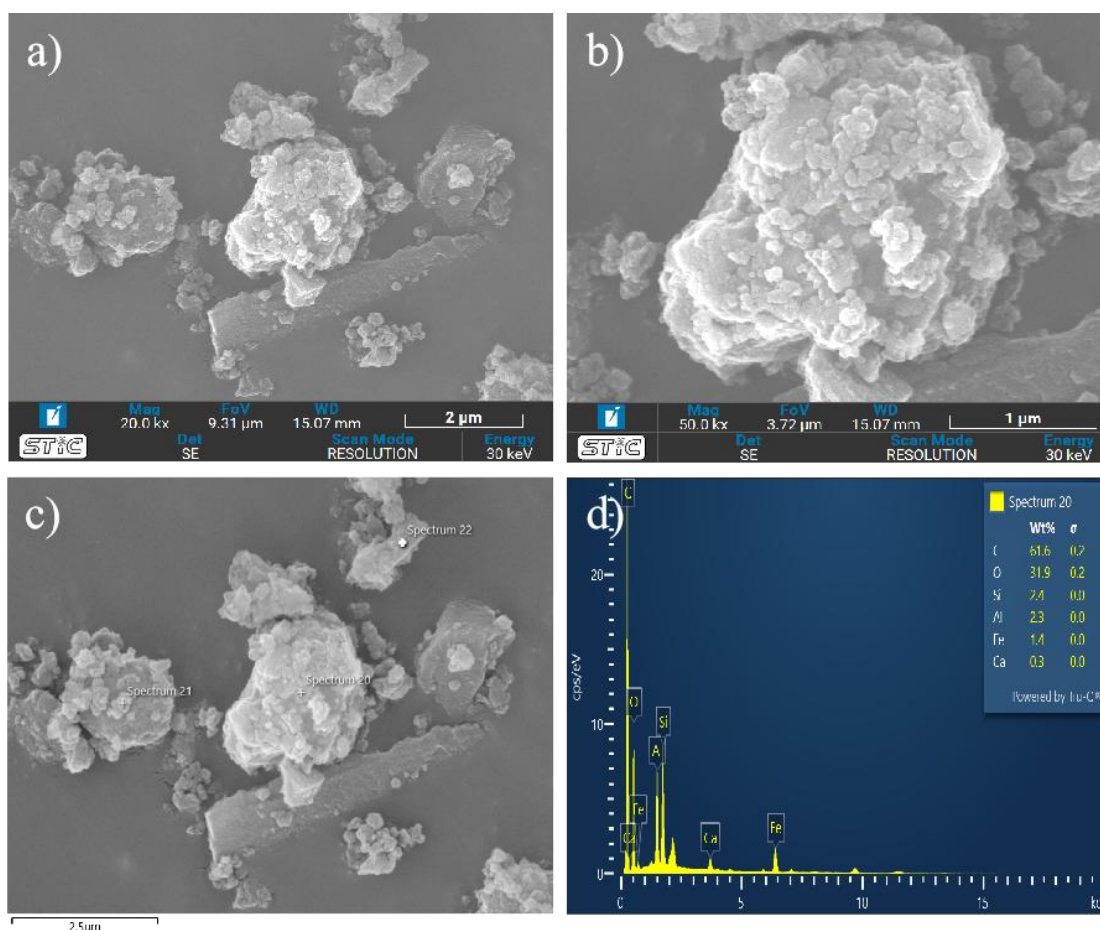
Figure 4. 8. SEM(a, b, c) and EDS (d) of the iron oxide extract from BA-Biomass Power Plant

4.4 Preparation Magnetic Mesoporous Silica for TC adsorption.

In the paper 1.(Appendices)
Revised paper after defensed thesis:
3.3. Adsorption Kinetics of TC on MMS
The adsorption kinetics explained the impact of time and temperature on the TC adsorption rate. The adsorption kinetics test was conducted by adding 0.03 g of adsorbent to 10 mL of 100 mg/L TC solution at 45 °C. The adsorption data were fitted using three popular kinetic models, including the pseudo-first-order, pseudo-second-order, and Elovich models. The kinetic models are listed in the Equations (9)–

(11) respectively, the corresponding nonlinear curves are shown in Figure 5, and Table 3 contains the estimated and shown kinetic parameters of TC adsorption on MMS.

$$Q_t = Q_e \left(1 - e^{-K_1 t}\right) \tag{9}$$

$$Q_t = \frac{K_2 Q_e^2 t}{1 + K_2 Q_e t} \tag{10}$$

$$Q_t = \left(\frac{1}{b}\right) ln(ab) + \left(\frac{1}{b}\right) ln(t); \tag{11}$$

where: Q_t : the adsorption capacity at t time (mg/g); t: time (min); K_1: the pseudo-first-order rate constant; K_2: the pseudo-second-order rate constant; a: the initial adsorption rate; b: the Elovich constant (g/mg)

Table 3. Adsorption Kinetic Coefficients.

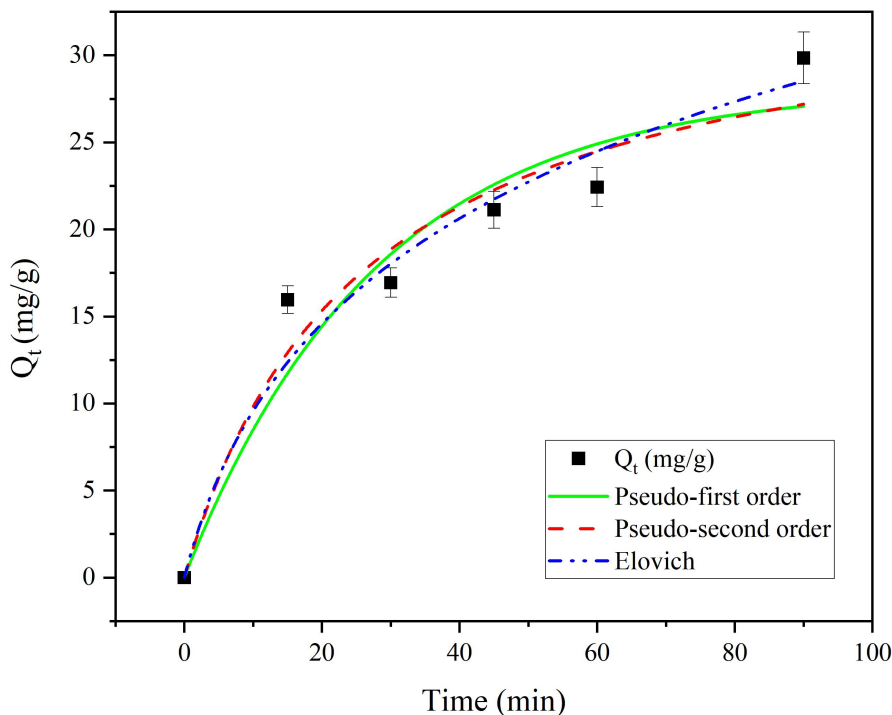| Model	Parameter	Value
pseudo-1st-order	K_1	0.04 ± 0.01
	Q_e	28.19 ± 3.70
	R^2	0.9266
	SSE	36.58
	χ^2	9.14
pseudo-2nd-order	Q_e	34.90 ± 5.62
	K_2	0.001 ± 0.0006
	R^2	0.9487
	SSE	25.54
	χ^2	6.38
Elovich	a	1.52 ± 0.02
	b	0.09 ± 0.0006
	R^2	0.9900
	SSE	526.01
	χ^2	0.52

Figure 5. Adsorption kinetics of TC onto MMS at 45 °C, with initial TC
concentration = 100 mg/L.

From the results presented in Table 3, it was possible to verify that the pseudo-2nd-order models have the determination coefficient (R^2) values higher and the error functions (SSE, and χ^2) lower than the pseudo-1st-order. Moreover, the Elovich model has the highest determination coefficient ($R^2 \approx 0.99$). However, the SSE values, commonly used as an indicator of model accuracy, are considerably high for this particular model [90], indicating this model is unable to explain the experimental data well. Consequently, the pseudo-2nd-order models were the best fit with the adsorption data.

4.5 Economic assessment

Table 4. 4 was displayed the calculate the cost of production for manufacturing 5kg from ashes, and calculates to expense for 1 kg.

The cost of producing the silica derived from ash as the raw material was found to be lower than that of the silica produced using silicate available on the market. With this study, the silica was obtained from ash, the production estimated cost for laboratory purpose is approximately $3.3739/kg. Comparing, the cost of a commercial SiO_2 sample reaches $5/kg as assumed.

Table 4. 4. Production cost for manufacturing 5kg

No.	Content	Quantity	Unit	Unit price ($)	Cost ($)
Raw materials cost					*12.75*
1	NaOH	20	kg	0.6	12
2	HCl 33%	2.5	L	0.3	0.75
3	Materials (ashes waste)	5	kg	0	0
Labour cost					*1.712*
4	Labour cost	1	process	8.56	1.712
Manufacturing cost					*2.4075*
5	Electricity used	18.05	kWh	0.15	2.4075
Total cost for 5kg					16.8695
Total cost for 1kg					3.3739

SiO_2 is the most important material used in many field industries. For examples, SiO_2 plays a crucial role in the semiconductor industry. It is used as an insulating material in integrated circuits (ICs) and serves as a gate oxide in metal-oxide-semiconductor (MOS) devices. As the demand for electronic devices continues to rise, reducing the cost of silicon dioxide is essential for making electronics more affordable. In addition, in the field of photovoltaics, SiO_2 is commonly used as an anti-reflective coating on solar cells. By reducing reflection losses, it enhances the overall efficiency of the solar panels. As solar energy becomes increasingly important for sustainable power generation, cost reduction in the manufacturing process is crucial for widespread adoption. Moreover, SiO_2 is a key component in the production of high-quality optical components, such as lenses, mirrors, and fibers. Its excellent optical properties and transparency make it an ideal material for various optical applications. Cost reduction in the manufacturing of these components can make optical devices and systems more affordable.

In summary, innovations in the production processes, resources of SiO_2 can lead to improved manufacturing efficiency, reducing energy consumption and waste generation. These advancements can help lower production costs and make products more cost-effective, resulting in cost savings for various sectors both in the present and the future.

CHAPTER 5. CONCLUSION AND FUTURE WORK

5.1 Conclusion

The study has shown the feasibility of utilizing the Biomass Power Plant and MSWI residues, namely bottom ash (BA) and Fly Ash (FA) as a source of silica and iron oxide. The hydrothermal process was studies to extract the maximum amount of amorphous silica and iron oxide, and the following conclusion was made:

- The BA and FA samples from Rubber Biomass Power Plant, and Municipal Solid Waste Incineration Plant in Southern, Thailand have successfully been applied in high purity silica obtained from raw material with low costs, which can be obtained by hydrothermal extraction.

- The highest yield of pure silica was achieved by re-fluxing at 90 °C in a sodium hydroxide solution 4M for 16 hours, with the ratio solid/liquid of 1:20 (g:L). Longer extraction times or higher ratios did not increase extraction efficiency.

- XRD and SEM analyses confirmed that the extracted silica had an amorphous structure, while FT-IR analysis indicated the presence of Si-O-Si bonds. The elemental composition showed that the extracted silica was 81 % pure. However, the separation capacity of iron oxide by acid washing from this sample was low quality and weak yield.

- MMS fabricated from rubber biomass power plant ash exhibited promise as a low-cost adsorbent for TC in aqueous solution.

- The maximum TC adsorption capacity of MMS was 276.74 mg/g at 60 °C. The pseudo-second-order model accurately described the adsorption kinetics, while the Langmuir model fitted the adsorption isotherms as well.

- Negative values of Gibbs free energy and enthalpy change confirmed that TC adsorption by MMS was spontaneous, and higher temperatures had an adverse effect on adsorption.

- MMS demonstrated excellent properties for TC removal, including high efficiency and easy separation from aqueous media by a magnet. It could also be utilized as an eco-friendly adsorbent for wastewater treatment.

- Generally, using incineration ash-derived waste as an SiO_2 source could decrease the costs of obtaining silica materials, and synthezing the new materials.

5.2 Implications in Thailand and Vietnam

Annually, hundreds of thousands of tons of ash are discharged from MSWI and biomass power plants in Thailand and Vietnam, yet most of it is not treated or efficiently reused. This is due to various reasons, including poor ash quality, lack of suitable treatment technology, inadequate awareness about environmental pollution and resource conservation, and insufficient policies and penalties. Currently,

the most common application for BA and FA is as a low-end aggregate in concrete, which still requires pretreatment due to contaminants. However, our study demonstrates the potential for utilizing MSWI and biomass power plant residues as a recycle-material to synthesize high-quality silica products and the MMS adsorbent. The extraction process eliminates many of the contaminants, leaving behind an inert residue that can be used in building materials. To apply these findings on an industrial scale, further research is needed to upscale the process and increase efficiency, as well as evaluate the economics in detail, including estimating the total investment cost, the discounted rate, the income tax, and the length of the project. Our study shows that recycling BA and FA into high-quality silica and a new adsorbent is a viable option including the technique and economic assessment.

5.3 Future work

● To encourage the growth of a sustainable market, it is essential to recognize the possibilities as well as the challenges associated with the recovery of valuable elements. The recovery of metals and silica from Biomass Power Plant and MSWI BA and FA can be used to offset the expenses of operating and maintaining active and legacy plants.

● There are few studies on the further purification of metals from ashes. Therefore, more research should be done on the further purification of metals. Additional extraction with solvent optimization with reference to the organic-to-aqueous ratio, to reduce secondary waste.

● Further study should concentrate on detailed economic analysis to contrast the price of heavy metals and silica technology with the value produced by recycling metals and making use of residual BA and FA. As well as estimating total investment cost and the factor effect to the manufacturing cost.

● Through life cycle analysis (LCA), examine the environmental advantages of precious elements recovery from ashes.

References

[1] E. Guanabara, K. Ltda, E. Guanabara, and K. Ltda, *What a Waste 2.0 : A Global Snapshot of Solid Waste Management to 2050. Washington, D.C.: World bank*. 2018.

[2] X. Dou *et al.*, "Review of MSWI bottom ash utilization from perspectives of collective characterization, treatment and existing application," *Renew. Sustain. Energy Rev.*, vol. 79, no. May 2016, pp. 24–38, 2017, doi: 10.1016/j.rser.2017.05.044.

[3] L. Makarichi, W. Jutidamrongphan, and K. anan Techato, "The evolution of waste-to-energy incineration: A review," *Renew. Sustain. Energy Rev.*, vol. 91, no. April, pp. 812–821, 2018, doi: 10.1016/j.rser.2018.04.088.

[4] C. J. Lynn, G. S. Ghataora, and R. K. Dhir OBE, "Municipal incinerated bottom ash (MIBA) characteristics and potential for use in road pavements," *Int. J. Pavement Res. Technol.*, vol. 10, no. 2, pp. 185–201, 2017, doi: 10.1016/j.ijprt.2016.12.003.

[5] P. H. Shih, J. E. Chang, and L. C. Chiang, "Replacement of raw mix in cement production by municipal solid waste incineration ash," *Cem. Concr. Res.*, vol. 33, no. 11, pp. 1831–1836, 2003, doi: 10.1016/S0008-8846(03)00206-0.

[6] and K. P. Thitipone Suwunwong, Sutthida Boonsamran, Kanchana Watla-iad, Patcharanan Choto, Nuttachat Wisittipanit, Tanan Chub-uppakarn, "Suitability and Characteristics of Combustion Residues from Renewable Power Plants for Subbase Agrregate Materials, in Thailand." pp. 2264–2278, 2021.

[7] Y. Han *et al.*, "Mesoporous Silica Derived from Municipal Solid Waste Incinerator (MSWI) Ash Slag : Synthesis , Characterization and Use as Supports for Au (III) Recovery," no. Iii, 2021.

[8] G. C. H. Doudart de la Grée, M. V. A. Florea, A. Keulen, and H. J. H. Brouwers, "Contaminated biomass fly ashes - Characterization and treatment optimization for reuse as building materials," *Waste Manag.*, vol. 49, pp. 96–109, 2016, doi: 10.1016/j.wasman.2015.12.023.

[9] R. Pode, "Potential applications of rice husk ash waste from rice husk biomass power plant," *Renew. Sustain. Energy Rev.*, vol. 53, pp. 1468–1485, 2016, doi: 10.1016/j.rser.2015.09.051.

[10] E. R. Teixeira, A. Camões, F. G. Branco, J. B. Aguiar, and R. Fangueiro, "Recycling of biomass and coal fly ash as cement replacement material and its effect on hydration and carbonation of concrete," *Waste Manag.*, vol. 94, pp. 39–48, 2019, doi: 10.1016/j.wasman.2019.05.044.

[11] S. Karnchanawong, T. Mongkontep, and K. Praphunsri, "Effect of green waste pretreatment by sodium hydroxide and biomass fly ash on composting process," *J. Clean. Prod.*, vol. 146, pp. 14–19, 2017, doi: 10.1016/j.jclepro.2016.07.126.

[12] A. K. Pote and V. V. Pande, "State of the Art Review on Emerging Applications of Mesoporous Silica Abstract :," pp. 12–20, 2020, doi: 10.2174/2666150002006010012.

[13] H. Misran, R. Singh, S. Begum, and M. Ambar, "Processing of mesoporous silica materials (MCM-41) from coal fly ash," vol. 186, pp. 8–13, 2007, doi: 10.1016/j.jmatprotec.2006.10.032.

[14] F. F. De Oliveira, K. O. Moura, L. S. Costa, C. B. Vidal, A. R. Loiola, and R. F. Nascimento, "Reactive Adsorption of Parabens on Synthesized Micro- and Mesoporous Silica from Coal Fly Ash : pH E ff ect on the Modi fi cation Process," 2020, doi: 10.1021/acsomega.9b03537.

[15] D. Chen *et al.*, "Municipal solid waste incineration residues recycled for typical construction materials—a review," *RSC Adv.*, vol. 12, no. 10, pp. 6279–6291, 2022, doi: 10.1039/d1ra08050d.

[16] V. N. Binh, N. Dang, N. T. K. Anh, L. X. Ky, and P. K. Thai, "Antibiotics in the aquatic environment of Vietnam: Sources, concentrations, risk and control strategy," *Chemosphere*, vol. 197, pp. 438–450, 2018, doi: 10.1016/j.chemosphere.2018.01.061.

[17] R. K. Pathak and A. K. Dikshit, "Effect of Various Environmental Parameters on Biosorptive Removal of Atrazine from WaterEnvironment," *Int. J. Environ. Sci. Dev.*, vol. 3, no. 3, pp. 289–293, 2012, doi: 10.7763/ijesd.2012.v3.233.

[18] D. Yang, "A Review in Tetracycline Removal from Water Environment by Carbon Nanotubes Adsorption," *IOP Conf. Ser. Earth Environ. Sci.*, vol. 721, no. 1, 2021, doi: 10.1088/1755-1315/721/1/012014.

[19] Q. Alam, "Valorization of Municipal Solid Waste Bottom Ash," vol. 1, no. 277, p. 149, 2019.

[20] "Biomass explained - U.S. Energy Information Administration (EIA)." https://www.eia.gov/energyexplained/biomass/ (accessed Apr. 08, 2023).

[21] V. Sawasdee and N. Pisutpaisal, "Rice Husk Ash Characterization and Utilization as a source of Silica Material," *Chem. Eng. Trans.*, vol. 93, no. March, pp. 79–84, 2022, doi: 10.3303/CET2293014.

[22] B. Thongma and S. Chiarakorn, "Recovery of silica and carbon black from rice husk ash disposed from a biomass power plant by precipitation method," *IOP Conf. Ser. Earth Environ. Sci.*, vol. 373, no. 1, 2019, doi: 10.1088/1755-1315/373/1/012026.

[23] L. Jiang *et al.*, "Influence of different demineralization treatments on physicochemical structure and thermal degradation of biomass," *Bioresour. Technol.*, vol. 146, pp. 254–260, 2013, doi: 10.1016/j.biortech.2013.07.063.

[24] G. Marland, "Accounting for Carbon Dioxide Emissions from Bioenergy Systems," *J. Ind. Ecol.*, vol. 14, no. 6, pp. 866–869, 2010, doi: 10.1111/j.1530-9290.2010.00303.x.

[25] B. Y. Chen and K. L. Lin, "Biotoxicity assessment on reusability of municipal solid waste incinerator (MSWI) ash," *J. Hazard. Mater.*, vol. 136, no. 3, pp. 741–746, 2006, doi: 10.1016/j.jhazmat.2006.01.009.

[26] "Waste-to-energy (MSW) in depth - U.S. Energy Information Administration (EIA)." https://www.eia.gov/energyexplained/biomass/waste-to-energy-in-depth.php (accessed Apr. 08, 2023).

[27] J. Zhai, I. T. Burke, and D. I. Stewart, "Beneficial management of biomass combustion ashes," *Renew. Sustain. Energy Rev.*, vol. 151, no. July, p. 111555, 2021, doi: 10.1016/j.rser.2021.111555.

[28] C. H. K. Lam, A. W. M. Ip, J. P. Barford, and G. McKay, "Use of incineration MSW ash: A review," *Sustainability*, vol. 2, no. 7, pp. 1943–1968, 2010, doi: 10.3390/su2071943.

[29] M. J. Quina, J. C. Bordado, and R. M. Quinta-Ferreira, "Treatment and use of

air pollution control residues from MSW incineration: An overview," *Waste Manag.*, vol. 28, no. 11, pp. 2097–2121, 2008, doi: 10.1016/j.wasman.2007.08.030.

[30] S. Kumar and D. Singh, "Municipal solid waste incineration bottom ash: a competent raw material with new possibilities," *Innov. Infrastruct. Solut.*, vol. 6, no. 4, pp. 1–15, 2021, doi: 10.1007/s41062-021-00567-0.

[31] M. Margallo, M. B. M. Taddei, A. Hernández-Pellón, R. Aldaco, and Á. Irabien, "Environmental sustainability assessment of the management of municipal solid waste incineration residues: A review of the current situation," *Clean Technol. Environ. Policy*, vol. 17, no. 5, pp. 1333–1353, 2015, doi: 10.1007/s10098-015-0961-6.

[32] G. C. C. Yang and T. Y. Yang, "Synthesis of zeolites from municipal incinerator fly ash," *J. Hazard. Mater.*, vol. 62, no. 1, pp. 75–89, 1998, doi: 10.1016/S0304-3894(98)00163-0.

[33] Y. Fan, F. S. Zhang, J. Zhu, and Z. Liu, "Effective utilization of waste ash from MSW and coal co-combustion power plant-Zeolite synthesis," *J. Hazard. Mater.*, vol. 153, no. 1–2, pp. 382–388, 2008, doi: 10.1016/j.jhazmat.2007.08.061.

[34] G. Chandrasekar, K. S. You, J. W. Ahn, and W. S. Ahn, "Synthesis of hexagonal and cubic mesoporous silica using power plant bottom ash," *Microporous Mesoporous Mater.*, vol. 111, no. 1–3, pp. 455–462, 2008, doi: 10.1016/j.micromeso.2007.08.019.

[35] Z. S. Liu, W. K. Li, and C. Y. Huang, "Synthesis of mesoporous silica materials from municipal solid waste incinerator bottom ash," *Waste Manag.*, vol. 34, no. 5, pp. 893–900, 2014, doi: 10.1016/j.wasman.2014.02.016.

[36] N. U. Amin, S. Khattak, S. Noor, and I. Ferroze, "Synthesis and characterization of silica from bottom ash of sugar industry," *J. Clean. Prod.*, vol. 117, pp. 207–211, 2016, doi: 10.1016/j.jclepro.2016.01.042.

[37] B. Ruiz, R. P. Girón, I. Suárez-Ruiz, and E. Fuente, "From fly ash of forest biomass combustion (FBC) to micro-mesoporous silica adsorbent materials," *Process Saf. Environ. Prot.*, vol. 105, pp. 164–174, 2017, doi: 10.1016/j.psep.2016.11.005.

[38] R. D. Alorro, S. Mitani, N. Hiroyoshi, M. Ito, and M. Tsunekawa, "Recovery of heavy metals from MSW molten fly ash by carrier-in-pulp method: Fe powder as carrier," *Miner. Eng.*, vol. 21, no. 15, pp. 1094–1101, 2008, doi: 10.1016/j.mineng.2008.02.005.

[39] M. Grosso, L. Biganzoli, and L. Rigamonti, "A quantitative estimate of potential aluminium recovery from incineration bottom ashes," *Resour. Conserv. Recycl.*, vol. 55, no. 12, pp. 1178–1184, 2011, doi: 10.1016/j.resconrec.2011.08.001.

[40] C. Ferna and E. S. Ingenieros, "Hydrometallurgical Recovery of Germanium from Coal Gasification Fly Ash .," *Ind Eng Chem Res*, vol. 47 (9), no. 3186–3191, pp. 3186–3191, 2008.

[41] T. Okada, Y. Tojo, N. Tanaka, and T. Matsuto, "Recovery of zinc and lead from fly ash from ash-melting and gasification-melting processes of MSW - Comparison and applicability of chemical leaching methods," *Waste Manag.*, vol. 27, no. 1, pp. 69–80, 2007, doi: 10.1016/j.wasman.2005.12.006.

[42] J. Tang and B. M. Steenari, "Leaching optimization of municipal solid waste incineration ash for resource recovery: A case study of Cu, Zn, Pb and Cd," *Waste Manag.*, vol. 48, pp. 315–322, 2016, doi: 10.1016/j.wasman.2015.10.003.

[43] T. Narukawa, K. W. Riley, D. H. French, and K. Chiba, "Speciation of chromium in Australian fly ash," *Talanta*, vol. 73, no. 1, pp. 178–184, 2007, doi: 10.1016/j.talanta.2007.03.003.

[44] Q. Wang, J. Yang, Q. Wang, and T. Wu, "Effects of water-washing pretreatment on bioleaching of heavy metals from municipal solid waste incinerator fly ash," *J. Hazard. Mater.*, vol. 162, no. 2–3, pp. 812–818, 2009, doi: 10.1016/j.jhazmat.2008.05.125.

[45] Y. pei Lan, Q. cai Liu, F. Meng, D. liang Niu, and H. Zhao, "Optimization of magnetic separation process for iron recovery from steel slag," *J. Iron Steel Res. Int.*, vol. 24, no. 2, pp. 165–170, 2017, doi: 10.1016/S1006-706X(17)30023-7.

[46] Z. Itam *et al.*, "Extraction of iron from coal bottom ash by carbon reduction method," *AIP Conf. Proc.*, vol. 2030, no. November, 2018, doi: 10.1063/1.5066902.

[47] Z. Itam *et al.*, "Extraction of metal oxides from coal bottom ash by carbon reduction and chemical leaching," *Mater. Today Proc.*, vol. 17, pp. 727–735, 2019, doi: 10.1016/j.matpr.2019.06.356.

[48] S. N. Aslipashaki, T. Khayamian, and Z. Hashemian, "Aptamer based extraction followed by electrospray ionization-ion mobility spectrometry for analysis of tetracycline in biological fluids," *J. Chromatogr. B*, vol. 925, pp. 26–32, 2013, doi: 10.1016/j.jchromb.2013.02.018.

[49] M. Cycoń, A. Mrozik, and Z. Piotrowska-Seget, "Antibiotics in the soil environment—degradation and their impact on microbial activity and diversity," *Front. Microbiol.*, vol. 10, no. MAR, 2019, doi: 10.3389/fmicb.2019.00338.

[50] S. I. Polianciuc, A. E. Gurzău, B. Kiss, M. Georgia Ștefan, and F. Loghin, "Antibiotics in the environment: causes and consequences," *Med. Pharm. Reports*, vol. 93, no. 3, pp. 231–240, 2020, doi: 10.15386/mpr-1742.

[51] I. Chopra and M. Roberts, "Tetracycline Antibiotics: Mode of Action, Applications, Molecular Biology, and Epidemiology of Bacterial Resistance," *Microbiol. Mol. Biol. Rev.*, vol. 65, no. 2, pp. 232–260, 2001, doi: 10.1128/mmbr.65.2.232-260.2001.

[52] S. H. Kim, H. K. Shon, and H. H. Ngo, "Adsorption characteristics of antibiotics trimethoprim on powdered and granular activated carbon," *J. Ind. Eng. Chem.*, vol. 16, no. 3, pp. 344–349, 2010, doi: 10.1016/j.jiec.2009.09.061.

[53] Y. Luo, L. Xu, M. Rysz, Y. Wang, H. Zhang, and P. J. J. Alvarez, "Occurrence and transport of tetracycline, sulfonamide, quinolone, and macrolide antibiotics in the haihe River basin, China," *Environ. Sci. Technol.*, vol. 45, no. 5, pp. 1827–1833, 2011, doi: 10.1021/es104009s.

[54] A. Javid, A. Mesdaghinia, S. Nasseri, A. H. Mahvi, M. Alimohammadi, and H. Gharibi, "Assessment of tetracycline contamination in surface and groundwater resources proximal to animal farming houses in Tehran, Iran," *J. Environ. Heal. Sci. Eng.*, vol. 14, no. 1, pp. 1–5, 2016, doi: 10.1186/s40201-016-0245-z.

[55] T. H. Le, C. Ng, N. H. Tran, H. Chen, and K. Y. H. Gin, "Removal of

antibiotic residues, antibiotic resistant bacteria and antibiotic resistance genes in municipal wastewater by membrane bioreactor systems," *Water Res.*, vol. 145, pp. 498–508, 2018, doi: 10.1016/j.watres.2018.08.060.

[56] G. Hamscher, S. Sczesny, H. Höper, and H. Nau, "Determination of persistent tetracycline residues in soil fertilized with liquid manure by high-performance liquid chromatography with electrospray ionization tandem mass spectrometry," *Anal. Chem.*, vol. 74, no. 7, pp. 1509–1518, 2002, doi: 10.1021/ac015588m.

[57] J. Tolls, "Sorption of veterinary pharmaceuticals in soils: A review," *Environ. Sci. Technol.*, vol. 35, no. 17, pp. 3397–3406, 2001, doi: 10.1021/es0003021.

[58] Z. Zhang, H. Li, and H. Liu, "Insight into the adsorption of tetracycline onto amino and amino–Fe3 + gunctionalized mesoporous silica: Effect of functionalized groups," *J. Environ. Sci. (China)*, vol. 65, pp. 171–178, 2018, doi: 10.1016/j.jes.2016.10.020.

[59] J. M. Lv, Y. L. Ma, X. Chang, and S. B. Fan, "Removal and removing mechanism of tetracycline residue from aqueous solution by using Cu-13X," *Chem. Eng. J.*, vol. 273, pp. 247–253, 2015, doi: 10.1016/j.cej.2015.03.080.

[60] L. Ji, W. Chen, L. Duan, and D. Zhu, "Mechanisms for strong adsorption of tetracycline to carbon nanotubes: A comparative study using activated carbon and graphite as adsorbents," *Environ. Sci. Technol.*, vol. 43, no. 7, pp. 2322–2327, 2009, doi: 10.1021/es803268b.

[61] H. Wang, H. Yao, P. Sun, J. Pei, D. Li, and C. H. Huang, "Oxidation of tetracycline antibiotics induced by Fe(III) ions without light irradiation," *Chemosphere*, vol. 119, pp. 1255–1261, 2015, doi: 10.1016/j.chemosphere.2014.09.098.

[62] C. Zhao, H. Deng, Y. Li, and Z. Liu, "Photodegradation of oxytetracycline in aqueous by 5A and 13X loaded with TiO2 under UV irradiation," *J. Hazard. Mater.*, vol. 176, no. 1–3, pp. 884–892, 2010, doi: 10.1016/j.jhazmat.2009.11.119.

[63] B. V. Chang, F. Y. Hsu, and H. Y. Liao, "Biodegradation of three tetracyclines in swine wastewater," *J. Environ. Sci. Heal. - Part B Pestic. Food Contam. Agric. Wastes*, vol. 49, no. 6, pp. 449–455, 2014, doi: 10.1080/03601234.2014.894784.

[64] M. A. Zazouli, H. Susanto, S. Nasseri, and M. Ulbricht, "Influences of solution chemistry and polymeric natural organic matter on the removal of aquatic pharmaceutical residuals by nanofiltration," *Water Res.*, vol. 43, no. 13, pp. 3270–3280, 2009, doi: 10.1016/j.watres.2009.04.038.

[65] Y. Xiang *et al.*, "Carbon-based materials as adsorbent for antibiotics removal: Mechanisms and influencing factors," *J. Environ. Manage.*, vol. 237, no. February, pp. 128–138, 2019, doi: 10.1016/j.jenvman.2019.02.068.

[66] D. W. Hawker, D. Chimpalee, P. Vijuksangsith, and M. Boonsaner, "The pH dependence of the cellulosic membrane permeation of tetracycline antibiotics," *J. Environ. Chem. Eng.*, vol. 3, no. 4, pp. 2408–2415, 2015, doi: 10.1016/j.jece.2015.08.012.

[67] M. J. Ahmed, "Adsorption of quinolone, tetracycline, and penicillin antibiotics from aqueous solution using activated carbons: Review," *Environ. Toxicol. Pharmacol.*, vol. 50, pp. 1–10, 2017, doi: 10.1016/j.etap.2017.01.004.

[68] E. K. Putra, R. Pranowo, J. Sunarso, N. Indraswati, and S. Ismadji, "Performance of activated carbon and bentonite for adsorption of amoxicillin from wastewater: Mechanisms, isotherms and kinetics," *Water Res.*, vol. 43, no. 9, pp. 2419–2430, 2009, doi: 10.1016/j.watres.2009.02.039.

[69] Y. Gao *et al.*, "Adsorption and removal of tetracycline antibiotics from aqueous solution by graphene oxide," *J. Colloid Interface Sci.*, vol. 368, no. 1, pp. 540–546, 2012, doi: 10.1016/j.jcis.2011.11.015.

[70] K. J. Choi, S. G. Kim, and S. H. Kim, "Removal of antibiotics by coagulation and granular activated carbon filtration," *J. Hazard. Mater.*, vol. 151, no. 1, pp. 38–43, 2008, doi: 10.1016/j.jhazmat.2007.05.059.

[71] Z. Li, L. Schulz, C. Ackley, and N. Fenske, "Adsorption of tetracycline on kaolinite with pH-dependent surface charges," *J. Colloid Interface Sci.*, vol. 351, no. 1, pp. 254–260, 2010, doi: 10.1016/j.jcis.2010.07.034.

[72] F. Yu, Y. Li, S. Han, and J. Ma, "Adsorptive removal of antibiotics from aqueous solution using carbon materials," *Chemosphere*, vol. 153, pp. 365–385, 2016, doi: 10.1016/j.chemosphere.2016.03.083.

[73] N. D. Mao *et al.*, "Biomass Fly Ash as an Alternative Approach for Synthesis of Amorphous Silica Nanoparticles with High Surface Area," *J. Nanosci. Nanotechnol.*, vol. 18, no. 5, pp. 3329–3334, 2017, doi: 10.1166/jnn.2018.14548.

[74] "About – PJT Technology Co.,Ltd." http://pjt.co.th/index.php/about/ (accessed May 15, 2023).

[75] T. Yala *et al.*, "Yala Biomass Power Plant Goes into Operation in Thailand," no. August 2003, 2006.

[76] V. K. Yadav, A. Amari, S. G. Wanale, H. Osman, and M. H. Fulekar, "Synthesis of Floral-Shaped Nanosilica from Coal Fly Ash and Its Application for the Remediation of Heavy Metals from Fly Ash Aqueous Solutions," *Sustain.*, vol. 15, no. 3, 2023, doi: 10.3390/su15032612.

[77] 杨卓舒 张磊 邝清林, "CN105776345A - Method for separating Fe2O3 in pulverized coal ash of pulverized coal furnace - Google Patents." https://patents.google.com/patent/CN105776345A/en (accessed Mar. 30, 2022).

[78] C. Azmiyawati, E. Sawitri, P. Siahaan, A. Darmawan, and L. Suyati, "Preparation of magnetite-silica-cetyltrimethylammonium for phenol removal based on adsolubilization," *Open Chem.*, vol. 18, no. 1, pp. 369–376, 2020, doi: 10.1515/chem-2020-0040.

[79] Y. Li *et al.*, "Preparation of magnetic mesoporous silica from rice husk for aflatoxin B1 removal: Optimum process and adsorption mechanism," *PLoS One*, vol. 15, no. 9 September, pp. 1–18, 2020, doi: 10.1371/journal.pone.0238837.

[80] S. Jabariyan and M. A. Zanjanchi, "A simple and fast sonication procedure to remove surfactant templates from mesoporous MCM-41," *Ultrason. Sonochem.*, vol. 19, no. 5, pp. 1087–1093, 2012, doi: 10.1016/j.ultsonch.2012.01.012.

[81] A. B. D. Nandiyanto, "Cost analysis and economic evaluation for the fabrication of activated carbon and silica particles from rice straw waste," *J. Eng. Sci. Technol.*, vol. 13, no. 6, pp. 1523–1539, 2018.

[82] G. D. Ulrich and P. T. Vasudevan, "How to estimate utility costs," *Chem. Eng.*, vol. 113, no. 4, pp. 66–69, 2006.

[83]   Y. Lu *et al.*, "Physical and chemical properties, pretreatment, and recycling of municipal solid waste incineration fly ash and bottom ash for highway engineering: A literature review," *Adv. Civ. Eng.*, vol. 2020, 2020, doi: 10.1155/2020/8886134.

[84]   D. An, Y. Guo, Y. Zhu, and Z. Wang, "A green route to preparation of silica powders with rice husk ash and waste gas," *Chem. Eng. J.*, vol. 162, no. 2, pp. 509–514, 2010, doi: 10.1016/j.cej.2010.05.052.

[85]   S. Saravanan and R. S. Dubey, "Synthesis of SiO2nanoparticles by sol-gel method and their optical and structural properties," *Rom. J. Inf. Sci. Technol.*, vol. 23, no. 1, pp. 105–112, 2020.

[86]   C. J. Lee, G. S. Kim, and S. H. Hyun, "Synthesis of silica aerogels from waterglass via new modified ambient drying," *J. Mater. Sci.*, vol. 37, no. 11, pp. 2237–2241, 2002, doi: 10.1023/A:1015309014546.

[87]   B. Shokri, M. A. Firouzjah, and S. I. Hosseini, "FTIR analysis of silicon dioxide thin film deposited by metal organic-based PECVD," *Proc. 19th Int. Plasma Chem. Soc.*, pp. 1–4, 2009, doi: www.ispc-conference.org.

[88]   S. Sankar *et al.*, "Biogenerated silica nanoparticles synthesized from sticky, red, and brown rice husk ashes by a chemical method," *Ceram. Int.*, vol. 42, no. 4, pp. 4875–4885, 2016, doi: 10.1016/j.ceramint.2015.11.172.

[89]   H. H. Mohamed and D. H. A. Besisa, "Eco-friendly and solar light-active Ti-Fe2O3 ellipsoidal capsules' nanostructure for removal of herbicides and organic dyes," *Environ. Sci. Pollut. Res.*, vol. 30, no. 7, pp. 17765–17775, 2023, doi: 10.1007/s11356-022-23119-0.

[90]   G. William Kajjumba, S. Emik, A. Öngen, H. Kurtulus Özcan, and S. Aydın, "Modelling of Adsorption Kinetic Processes—Errors, Theory and Application," *Adv. Sorption Process Appl.*, pp. 1–19, 2019, doi: 10.5772/intechopen.80495.

Appendices

Paper 1: Hanh, P.T.H.; Phoungthong, K.; Chantrapromma, S.; Choto, P.; Thanomsilp, C.; Siriwat, P.; Wisittipanit, N.; Suwunwong, T.Adsorption of Tetracycline by Magnetic Mesoporous Silica Derived from Bottom Ash—Biomass Power Plant. Sustainability 2023, 15, 4727. https://doi.org/10.3390/su15064727

sustainability

Article

Adsorption of Tetracycline by Magnetic Mesoporous Silica Derived from Bottom Ash—Biomass Power Plant

Phan Thi Hong Hanh [1], Khamphe Phoungthong [1], Suchada Chantrapromma [2], Patcharanan Choto [3,4], Chuleeporn Thanomsilp [3], Piyanuch Siriwat [3], Nuttachat Wisittipanit [3,5] and Thitipone Suwunwong [3,4,*]

[1] Industrial Ecology in Energy Research Center, Faculty of Environmental Management, Prince of Songkla University, Songkhla 90112, Thailand
[2] Division of Physical Science, Faculty of Science, Prince of Songkla University, Songkhla 90112, Thailand
[3] School of Science, Mae Fah Luang University, Chiang Rai 57100, Thailand
[4] Center of Chemical Innovation for Sustainability, Mae Fah Luang University, Chiang Rai 57100, Thailand
[5] Department of Materials Engineering, School of Science, Mae Fah Luang University, Chiang Rai 57100, Thailand
* Correspondence: thitipone.suw@mfu.ac.th; Tel.: +66-869658254

Abstract: In recent years, the contamination of the aquatic environment with antibiotics, including tetracyclines, has drawn much attention. Bottom ash (BA), a residue from the biomass power plant, was used to synthesize the magnetic mesoporous silica (MMS) and was utilized as an adsorbent for tetracycline (TC) removal from aqueous solutions. The MMS was characterized by Fourier transform-infrared (FTIR), X-ray diffraction (XRD) pattern, and scanning electron microscopy (SEM). Optimum conditions were obtained in overnight incubation at 60 °C, a pH of 6–8, and an adsorption capacity of 276.74 mg/g. The isotherm and kinetic equations pointed to a Langmuir isotherm model and pseudo-first-order kinetic optimum fitting models. Based on the very low values of entropy changes ($\Delta S°$), the negative value of enthalpy changes ($\Delta H°$) (-15.94 kJ/mol), and the negative Gibbs free-energy changes ($\Delta G°$), the adsorption process was physisorption and spontaneous.

Keywords: antibiotic contamination; tetracycline; solid waste; adsorption mechanisms

check for updates

1. Introduction

Antibiotics have been commonly used for the prevention and treatment of infectious diseases, both in humans and animals. According to Cycon et al., the situation analyzed in 75 countries, indicates that the antibiotics usage climbed by 65%, and the prediction is that in 2030, the consumption of antibiotics will be higher by 200% compared with 2015 [1]. Among antibiotics, tetracycline (TC) is a conventional, inexpensive antibiotic having wide-ranging antibacterial action that is frequently used in both human and veterinary medicine to prevent infection [2]. Additionally, TC antibiotics are utilized as a growth stimulant for animals and for agricultural purposes [3,4]. Moreover, TC constitutes one of the most important antibiotic families, ranking second in production and usage worldwide [5,6]. Because of its high aqueous solubility, TC has been found in ecological communities such as surface water and groundwater (ranging from 5.4 to 8.1 ng/L) [7], municipal solid waste (greater than 100 ng/L) [8], and soil (ranging from 86.2 to 198.7 µg/kg) [9], and it can be easily transferred to other environments via aqueous matrixes [10], and like other antibiotics, it has a structural framework called naphthol ring that makes it difficult to degrade [11]. Thus, Cycon et al. [1] suggested that "the reason is that antibiotics are not completely metabolized by humans and animals, and a large proportion of the administered drug is released as the parent compound through feces and urine, discharging into domestic wastewater and into the pits where slurries/sludges are deposited". Gu and Karthikeyan [12] also found that "in the statewide survey of wastewater treatment plants, the compound TC was the most frequently detected antibiotic (among 25 antibiotics), being present in 80% of the

wastewater influent and effluent samples". However, standard aqueous solution water treatment and spontaneous biodegradation are ineffective in removing TC from aqueous solution [12,13]. Therefore, techniques for the secure and efficient removal of TC from liquid have received a great deal of interest. Methods for TC removal include oxidation [14], photo electrocatalytic [15], degradation [16], membrane processing [17], adsorption [18], permeation [19], flocculation [19], ozonation oxidation [19]. Among these, adsorption has several advantages over other procedures, including ease of operation, inexpensive operating costs, and significant removal efficiency at extremely low TC content in wastewater and water [20]. Particularly, no generation of toxicity of intermediated and by-products during adsorption makes it a more attractive appealing method of treating TC [21]. Until now, some studies investigated the adsorption and removal of tetracyclines on several materials such as graphene oxide [22], activated carbon [23], kaolinite [24], single-walled carbon nanotubes, and multi-walled carbon nanotubes [13]. Carbon nanotubes and graphene, which have a high graphite structure, have a strong TC elimination capacity [25]. However, the high manufacturing, disposal, and regeneration costs of the aforementioned materials would pose significant barriers in their practical application for TC adsorption, as well as the capacity for large-scale application. As a result, there is still a considerable desire for the development of efficient and affordable, simple-to-operate, high-selectivity devices.

Mesoporous silicas are often employed in a variety of applications, including catalysis, separation, drug administration, chemical sensing, optic and electrical devices, rubber reinforcement, and as a template in the production of nanomaterials [26]. Because they possess a large surface area, big pore size, pore volume, and regular channel-type structures, these properties are potential advantages that suit the adsorbate. A renewed interest in the design of adsorbents [27] and catalysts has been sparked by the discovery of hexagonally organized mesoporous silica [28], which has a distinctively large surface area, well-defined pore size, and pore-shaped pores. For the production of surfactant-template silica materials, which need an organic structure-directing agent or template is typically a single surfactant, such as: the Pluronic-type surfactant; poly(ethylene oxide)-b-poly(propylene oxide)-b-poly(ethylene oxide)-Pluronic P123 ($EO_{20}PO_{70}EO_{20}$) or Pluronic F127 ($EO_{106}PO_{60}EO_{106}$) and cetyltrimethylammonium bromide (CTMAB) [29–32]. Some studies have magnetized the silicates to allow for rapidly and effectively separating the adsorbents from the aqueous solution by an external magnetic field, and incorporating magnetic elements within or on mesoporous silicates has also enhanced the adsorption properties [33].

Some previous researches have investigated magnetic mesoporous silica (MMS) with a variety of structures: including embedded [31], core-shell [32], and yolk-shell [34]. The MMS could be synthesized by combining the mesoporous silica (MS) and magnetic particles. Tetraethyl orthosilicate (TEOS) was used as the silica source, and magnetic particles were prepared from iron (II) chloride tetrahydrate ($FeCl_2,4H_2O$), iron (III) chloride hexahydrate ($FeCl_3 \cdot 6H_2O$) [35]. Because TEOS is expensive and magnetic particles require time and chemicals to make, searches for alternative cheap source are necessary.

Bottom ash (BA)—biomass power plant was a byproduct from the combusting of agricultural waste to produce energy. Approximately 85–95 percent of BA was generated from biomass power plants [36], with SiO_2 making up the majority of this ash [37]. Thus, these residues were an ideal silica source. Currently, Thailand has an abundance of BA—biomass power plants that may be utilized to create magnetic mesoporous silica as an appropriate supply. Generally, utilizing the residues from incineration and combustion plant to produce silica materials is feasible. Some studies have been successful in converting this byproduct to zeolite in alkali solution [38], synthesizing zeolitic material and successfully separating SiO_2 from municipal solid waste incineration (MSWI) ash [39], MCM-41, SBA-15, and SBA-16 mesoporous silica from power plant bottom ash were successfully synthesized for the first time in 2007 [40]. Mesoporous silica was prepared by the sol-gel method from municipal solid waste incineration bottom ash [41] and industrial fly ash [42]. This application would increase the usage of BA—biomass power plants, minimize pollution, and effectively improve the quality of the wastewater process. However, according to our

knowledge, there has not been any published research on the synthesis of magnetic silica nanoparticles derived from BA for specific applications in the adsorption of tetracycline.

Therefore, the purpose of this study is to apply magnetic mesoporous silica synthesized from biomass power plant ash to absorb TC from aqueous solutions. The properties of the MMS including surface area, function groups, and crystal structure were analyzed. The research was conducted on the isotherm model, kinetics model, and thermodynamic characteristics of TC's adsorption onto the MMS. According to the findings of adsorption tests, the MMS demonstrated promising potential for TC removal from water. This study provides a detailed technique for achieving the goal of treating trash with waste in addition to describing how solid waste is utilized as a resource.

2. Materials and Methods

2.1. Materials

In this study, the bottom ash (BA) was obtained from the rubber biomass power plant of Gulf Yala company, Yala, located in southern Thailand. The composition of BA was determined by X-ray fluorescence spectrometer (XRF) as listed in Table S1 (in the Supplementary material). Tetracycline hydrochloride, 96%, Alfa Aesar were used without further purification. Hexadecyltrimethyl ammonium bromide (CTAB) $\geq$ 98%, Sigma, Cibolo, TX, USA; Sodium hydroxide (NaOH) 98%, Loba Chemie PVT.LTD, India; Hydrochloric acid (HCl) 37%, Qrec, Newzealand; Ethanol 99.9%, Qrec, Newzealand.

2.2. Methods

2.2.1. Synthesis of Magnetic Mesoporous Silica

The biomass power plant ash (BA) which includes 55% SiO_2 content as the main component (Table S1 in the Supplementary Material) was used as raw material for extraction of SiO_2 compound. Briefly, BA sample was ground into small particles (<45 μm) and then washed with DI water several times and dried in the oven at 90 °C for 24 h. The permanent magnets were employed to separate the magnetic and nonmagnetic ashes. The magnetic ash was served as the magnetic component in the magnetic mesoporous silica, and the nonmagnetic ash was utilized to extract silica. The weight ratio between the magnetic and nonmagnetic ashes was 1:10.

A total of 4 g of nonmagnetic ash was refluxed with 100 mL NaOH solution with the concentration 4 M at 90 °C for 16 h in a round bottom flask. Then, the reaction solution was filtered through a membrane of 0.45 μm and the supernatant was collected for adjusting pH at 7 by 5 M HCl and aging at the room temperature for 24 h. The precipitated product was washed with distilled water several times and dried at 90 °C for 24 h. To prepare the sodium silicate solution, the obtained white power and NaOH (4:5 w/w) were precisely weighed and then dissolved in 250 mL of distilled water at 80 °C for 1 day [43]. The white power is SiO_2 and was extracted from BA, which was analyzed by X-ray fluorescence spectrometer (XRF), as shown in Table S2 (in the Supplementary material).

Deionized water (20 mL) was added to 1.2 g hexadecyltrimethyl ammonium bromide (CTAB) and then mixed at 40 °C until a clear solution was observed. The aqueous CTAB solution was slowly mixed with sodium silicate solution and continuously stirred for 15 min. This mixture was added slowly into the magnetic ash; the ratio of the mass of maghemite to Na_2SiO_3 10% was 1:20, and it was stirred while being heated to 80 °C. After further stirring for 30 min, the pH of the mixture was adjusted to 11 by 5 mol/L HCl solution and then continuously stirred for 6 h. The mixture was kept in a water bath at 80 °C for 72 h. The ethanol 99.9%, 100 mL, was added to the precipitated product. To eliminate CTAB, the mixture was sonicated for 30 min at 60 °C [44] and then washed with DI water several times and dried at 80 °C for 24 h.

The experimental procedure was repeated more than three times to verify that the results are reproducible.

2.2.2. Characterization

The mineral compositions in BA and MMS were determined by X-ray fluorescence (XRF), (S2175 Ranger, Bruker, Burladingen, Germany). Fourier transform infrared spectroscopy FT-IR (Perkin Elmer Model Spectrum GX) was used to analyze the specific functional groups of the adsorbents by compressed samples into KBr pellets and then analyzed with a Nicole IS10 spectrometer over the wavelength ranged from 400 to 4000 cm^{-1}. X-ray diffraction (XRD) pattern (PAN analytical, X'Pert Pro MPD) was performed on a Bruker AXS Advance instrument for confirmation the structure. The surface morphology (SEM) of magnetic mesoporous silica was examined by scanning electron microscopy (SEM, Apreo, FEI, South Moravian Region, Czech Republic) running by Schottky field emission at the accelerating voltage of 20 kV in high vacuum mode. The elemental mapping analysis of the sample was recorded by energy-dispersive X-ray spectrometer (EDS)—(X-Max80, Oxford, UK).

2.2.3. Adsorption Experiments

MMS was used for tetracyclines (TC) adsorption in an aqueous solution. To find the ideal conditions, the impact of adsorption time and temperature on the unit adsorption capacity and adsorption rate of TC was investigated. MMS (3 mg) was dispersed in a flask containing 10.0 mL TC solution with various concentrations (10–100 mg/L), pH 6–8, and then fully homogenized with a vortex mixer. The suspension was incubated overnight at 25 °C, 45 °C, and 60 °C and covered with aluminum foil to protect TC from the potential photo degradation. MMS was then separated from the samples through a magnet after centrifuging at 2000 rpm for 15, 30, 45, 60, and 90 min while maintaining the experiment temperature including centrifugation. The residual concentration of TC in an aqueous solution was determined by UV–vis absorbance at 357 nm, using a calibration curve built. All the experiments were replicated thrice, and the averaged results were reported. Equation (1) was used to calculate the percentage removal of TC, and Equation (2) was used to determine the adsorption capacity:

$$Removal(\%) = \frac{(C_o - C_e)}{C_o} \times 100 \tag{1}$$

$$Q_e = \frac{(C_o - C_e) \times V}{m} \tag{2}$$

where:

- Q_e is the amount of TC adsorption per unit weight of adsorbent (mg/g);
- C_o is the initial concentration of TCs (mg/mL);
- C_e (mg/L) is the equilibrium concentration of TC;
- V is the solution volume (mL);
- m is the mass of adsorbent (g).

3. Results and Discussion

3.1. Characterization of MMS

The FT-IR peaks of the MMS before and after adsorption of TC were collected in the range from 400 to 4000 cm^{-1} (Figure 1), indicating the chemical bonds and functional groups in the compound. The O–H stretching vibration was identified as the source of the big broadband at 3440 to 3443 cm^{-1}. The absorption peaks at 1640 cm^{-1} were caused by the symmetric and asymmetric bending vibration of C=O. Fe–O stretching was assigned to the band below 700 cm^{-1}. The characteristic absorption bands of the sample at 692 and 583 cm^{-1} were assigned to iron(II) oxide bending, and the band at 459 to 446 cm^{-1} was ascribed to the bending vibration mode of Fe$_2$O$_3$. The band at 1048 cm^{-1} to 1051 cm^{-1}, which is associated with Si-O-Si antisymmetric stretching vibrations, is a sign that silicon dioxide is present in the sample. The bands at 579 and 583 cm^{-1} are also an indication of the presence of Si–O–Fe [45]. Most of the adsorbent's peaks remained constant after TC

adsorption, revealing that the adsorption procedure did not modify the structure of material. However, several distinctive peaks at 1478, 2852, and 2922 cm^{-1} were characteristic peaks of the C=C skeleton and C-H stretching vibration of CH_2 and CH_3 induced by aromatic groups of TC [46,47]. The FT-IR spectrum proved that TC was adsorbed onto the adsorbent and the sample's structure is mostly stable after adsorption [48].
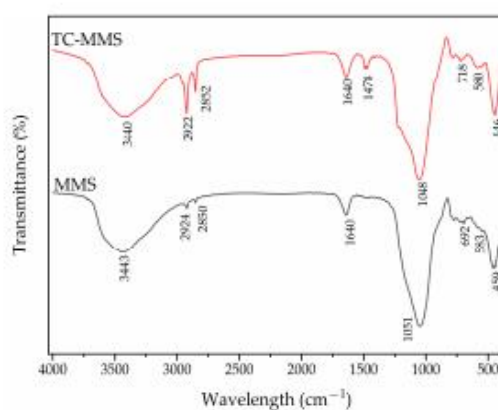

Figure 1. FTIR spectra of the adsorbent before and after adsorption of TC.

The XRD profile of the MMS in the FT-IR spectrum proved that TC was adsorbed onto the adsorbent and the sample's structure is mostly stable after adsorption [48].

Comparisons with those of SiO_2 (extracted from biomass power plant Ash) and Fe_2O_3 peak [49] are shown in Figure 2. The XRD pattern of the MMS exhibited the characteristic diffraction peaks of Fe_2O_3 with weak intensity due to the lower concentration of Fe_2O_3. In addition, the relatively slightly broad peak observed at 15−30° arose from the SiO_2, demonstrating that the crystalline structure of the iron oxide was retained after the encapsulation in silica.
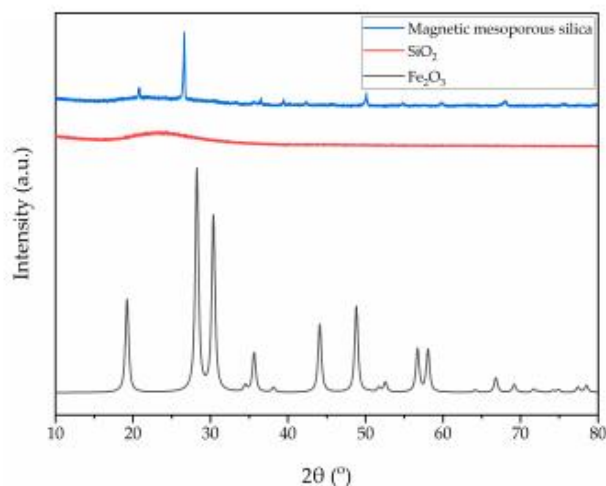

Figure 2. XRD patterns of the MMS.

The morphological structures of the MMS were examined using SEM. As shown in Figure 3a, there are many unobvious spherical particles (aggregated) with a size of around 50−80 nm. A rough surface, which mainly consists of not−well−crystallized Fe$_2$O$_3$, seems not to be efficient to achieve homogeneous coating SiO$_2$, but instead irregular and severely agglomerated particles are observed in Figure 3b,c.
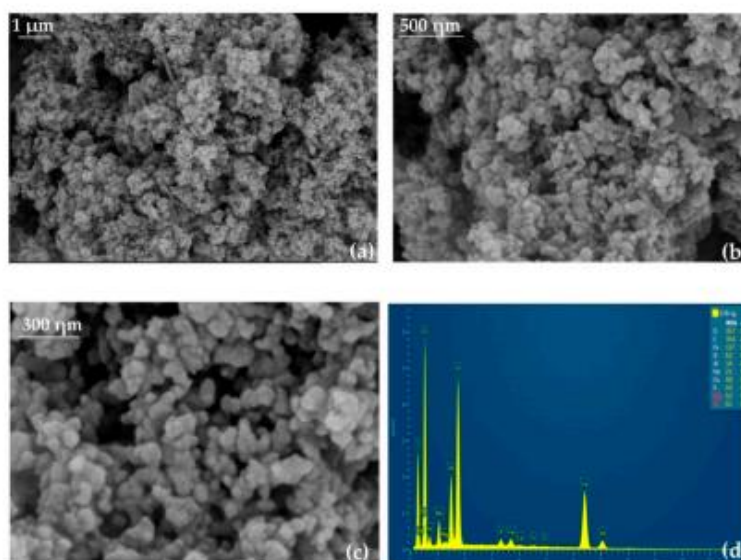

Figure 3. SEM images of MMS (a–c), and EDS curve of MMS (d).

The samples typically determined the elemental analysis or chemical properties using energy-dispersive X−ray spectrometry (EDS). The various elements in the sample are represented by energy peaks. As-prepared nanocomposites were found to include significant amounts of Fe, O, Si, Ti, Na, Ca, Al, etc. (Figure 3d), confirming the formation of additional nanocrystals on the surface of Fe$_2$O$_3$@SiO$_2$ particles.

3.2. Adsorption Isotherms of TC on MMS

In order to elucidate the interactions between the adsorption ability of the MMS and TC in solution at adsorption equilibrium, the data were modeled using four adsorption isotherms, including Langmuir, Freundlich, Temkin, and Sips isotherm models at 25, 45, and 60 °C. The isotherm models were listed below with Equations (3)–(6) as follows.

$$Q_e = \frac{Q_m K_L C_e}{1 + K_L C_e} \; ; \; R_L = \frac{1}{1 + K_o C_o} \tag{3}$$

$$Q_e = K_f C_e^{\frac{1}{n}} \tag{4}$$

$$Q_e = \frac{RT}{b_T} ln(K_T C_e) \tag{5}$$

$$Q_e = Q_m \frac{(K_S C_e)^a}{1 + (K_S C_e)^a} \tag{6}$$

where Q_m = maximum adsorption ability (mg/g), C_e = equilibrium concentration (mg/L), Q_e = adsorption capacity (mg/g) at equilibrium time, K_L = Langmuir constant, R_L = separation constant, K_f and n = Freundlich constant, R = universal gas constant (8.314 J/mol),

T = temperature in terms of Kelvin, b_T = Temkin constant, K_T = equilibrium bond constant related to the maximum energy of bond, and K_s and a are Sips constants.

According to Figure 4a, as the equilibrium TC concentration climbed, the TC's capacity to adsorb on the MMS also dramatically increased. It was determined that the adsorption process was endothermic because the adsorption capacity of TC increased as the adsorption temperature rose. This is likely because the higher temperature supported the quantity of activated functional groups on the surface of the MMS or sped up the diffusion rate of the tetracycline molecules.
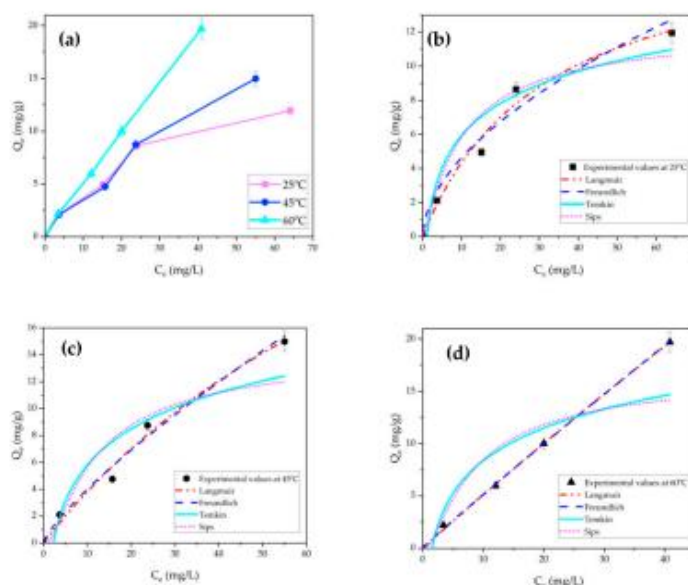

Figure 4. Adsorption isotherms of TC onto MMS at 25, 45, and 60 °C (a), The nonlinear fits for Langmuir, Freundlich, Temkin, Sips models at 25 °C (b), 45 °C (c), 60 °C (d). (adsorbent dosage = 0.03 g/L, pH = 8, V = 10 mL).

The starting TC concentration used in the modeling procedure varied from 10 to 100 mg/L, and the adsorption temperature was adjusted at 25, 45, and 60 °C. Figure 4b–d show the plot of the nonlinear fits for the aforementioned four isotherm models, and Table 1 lists the related parameter values. The Langmuir model was more appropriate to explain the adsorption of TC onto the MMS, as shown by the correlation coefficients, R^2, which were consistently close to 1 and the sum of square error (SSE), chi-square (χ^2) values, which suggest that the surface of the MMS was homogeneous and the adsorption was monolayer. Additionally, K_L is a significant evaluation factor in relation to the binding site affinities. The value of K_L was between 0–1 and declined with the rising temperature, and separation factor (R_L) <1 reflected that the adsorption of TC onto the MMS was favorable [50]. The nonlinear fitting of the Langmuir model (Figure 4b) showed the adsorption capacity (Q_m) of MMS for TC was 276.74 mg/g.

Table 1. Parameters of adsorption isotherm model of TC onto MMS at 25, 45, 60 °C.

Temp (°C)	25 °C	45 °C	60 °C
		Langmuir	
Q_m	18.11 ± 2.65	43.92 ± 15.67	276.74 ± 159.62
K_L	0.031 ± 0.009	0.009 ± 0.004	0.002 ± 0.001
R^2	0.9832	0.9876	0.9815
SSE	1.58	1.74	0.19
χ^2	0.53	0.53	0.53
		Freundlich	
n	0.54 ± 0.003	0.79 ± 0.001	$0.96 \pm 3.25 \times 10^{-4}$
K_F	1.31 ± 0.01	0.64 ± 0.003	$0.56 \pm 6.20 \times 10^{-4}$
R^2	0.9867	0.9983	0.9999
SSE	138.27	32.07	1.66
χ^2	0.14	0.03	0.002
		Temkin	
A_T	0.58 ± 0.01	0.58 ± 0.01	0.88 ± 0.03
B_T	790.61 ± 7.53	790.62 ± 7.53	909.52 ± 10.28
R^2	0.9181	0.9181	0.8880
SSE	855.40	3806.77	8002.25
χ^2	0.86	3.89	8.03
		Sips	
Q_m	12.92 ± 0.11	14.52 ± 0.17	17.07 ± 0.24
K_S	0.18 ± 0.02	0.35 ± 0.08	0.47 ± 0.13
A	2.09 ± 0.18	3.79 ± 0.77	3.63 ± 0.87
R^2	0.9603	0.9415	0.9218
SSE	512.81	1055.65	2210.77
χ^2	0.51	1.06	2.22

The R^2 values of the Freundlich isotherms were from 0.98 to 0.99, but the $1/n$ values were more than 1, at 1.85, 1.26, and 1.04, with increased temperatures at 25, 45, 60 °C, respectively, suggesting the adsorption is not prone to occur. Therefore, the Freundlich isotherm had a hard time accurately explaining the TC adsorption pattern.

The Temkin and Sips isotherms were a poor fit, although heterogeneity was also assumed. The Temkin isotherms illustrate that the heat of adsorption is negatively proportional to the surface area covered by the adsorbate molecules. The Temkin's constant, abbreviated B_T, represents the heat generated during adsorption. The fact that B_T was positive (790.61–909.52 J/mol) for the TC adsorption from the aqueous solution indicates that TC was endothermically adsorbed on the MMS. The equilibrium binding constant A_T is the quantity that relates to the greatest binding energy. When the temperature was raised from 25 to 60 °C, the values of A_T also increased from 0.58 to 0.88 L/mg, indicating that the adsorption of TC on the MMS was endothermic.

Equations (7) and (8) of the van't Hoff equation were used to compute the Gibbs free-energy change $\Delta G°$ enthalpy $\Delta H°$ and entropy $\Delta S°$ during the adsorption process (8). The results are displayed in Table 2.

$$\Delta G° = -RTlnK_L \tag{7}$$

$$ln(K_L) = \frac{\Delta S°}{R} - \frac{\Delta H°}{RT} \tag{8}$$

where R is the ideal gas constant 8.314 J/(mol·K), T is Kelvin temperature (K), and K_L is the Langmuir isotherm equilibrium constant (L/mg) [50–53].

Table 2. Thermodynamic parameters of TC adsorption onto MMS.

Temperature (K)	$\Delta G°$ (kJ/mol)	$\Delta H°$ (kJ/mol)	$\Delta S°$ (J/(mol.K)
298	−23.61		
318	−21.92	−7.62	−15.94
333	−18.79		

The absolute values of $\Delta G°$ are negative for all the parameter intervals, indicating that the adsorption behavior is spontaneous. $\Delta G°$ also increased as the adsorption temperature rose, suggesting that the adsorption process was impeded [51]. Moreover, the value of $\Delta G°$ in the range from −20 to −80 (kJ/mol) showed that physisorption was involved in the process, but a minor chemical action effect could speed up the procedure. Furthermore, the value of $\Delta H°$ lower than 20 (kJ/mol) revealed the physical adsorption with van der Waals interaction implied in the process mechanism [52]. A very low $\Delta S°$ value (−15.94 J/(mol.K)) proved a little change in entropy occurred during the adsorption of TC by the MMS [53].

3.3. Adsorption Kinetics of TC on MMS

The adsorption kinetics explained the impact of time and temperature on the TC adsorption rate. The adsorption kinetics test was conducted by adding 0.03 g of adsorbent to 10 mL of 100 mg/L TC solution at 45 °C. The adsorption data were fitted using three popular kinetic models, including the pseudo-first-order, pseudo-second-order, and Elovich models. The kinetic models are listed in the Equations (9)–(11) respectively, the corresponding nonlinear curves are shown in Figure 5, and Table 3 contains the estimated and shown kinetic parameters.

$$Q_t = Q_e \left(1 - e^{-K_1 t}\right) \tag{9}$$

$$Q_t = \frac{K_e Q_e^2 t}{1 + K_2 Q_e t} \tag{10}$$

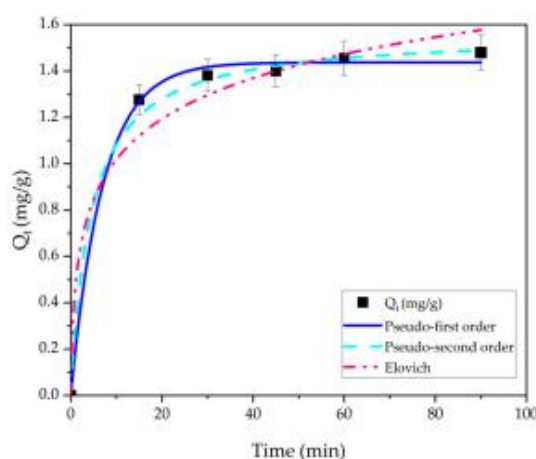$$Q_t = \left(\frac{1}{b}\right) In(ab) + \left(\frac{1}{b}\right) In(t); \tag{11}$$

Figure 5. Adsorption kinetics of TC onto MMS at 45 °C, with initial TC concentration = 100 mg/L.

Table 3. Adsorption Kinetic Coefficients.

Model	Parameter	Value
pseudo-1st-order	K_1	0.14 ± 0.02
	Q_e	1.44 ± 0.02
	R^2	0.9971
	SSE	0.005
	χ^2	0.00
pseudo-2nd-order	Q_e	1.56 ± 0.003
	K_2	0.14 ± 0.002
	R^2	0.9646
	SSE	2.44
	χ^2	0.00
Elovich	β	1.33 ± 0.05
	α	3.90 ± 0.03
	R^2	0.9559
	SSE	4.20
	χ^2	4.20

For the pseudo-second-order and Elovich models, R^2 was considerably less than 1, and SSE, χ^2 were higher. It was determined that neither model could adequately explain the experimental findings. However, the pseudo-first-order kinetic model showed a high value of R^2 (0.9971) and a small value of SSE, χ^2. The closer fitting curves imply that the pseudo-first-order adsorption process was dominant for TC adsorption on the MMS.

As presented in Table 4, the MMS has a high adsorption capacity when compared to the Q_m values of a variety of adsorbents utilized from waste for TC antibiotics in aquatic environments. From this table, the MMS can be considered as an alternative adsorbent material for TC adsorption.

Table 4. The capacity adsorption of TC with other different adsorbents' utilization from waste.

Adsorbent	Q_m (mg g^{-1})	Refs.
Alkali modified magnetic biochar (MSBC)	97.962	
Alkali-acid modified magnetic biochar (MSABC)	98.334	[54]
The raw biochar (RBC)	37.803	
Alfalfa-derived biochar	372	[55]
Pinus taeda-derived activated biochar	274.8	[56]
Waste chicken-feather-derived multilayered graphene-phase biochar	388.33	[57]
Clay-biochar composites	77.962	[58]
Spent coffee-ground-derived biochar	39.22	[59]
Biomass ash pyrolyzed from municipal sludge	50.75	[60]
Shrimp Shell Waste	229.98	[61]
Magnetic mesoporous silica from BA-Biomass Power Plant	276.74	In this study

4. Conclusions

Magnetic mesoporous silica that was fabricated from rubber biomass power plant ash was considered as a low-price adsorbent for tetracycline adsorption in aqueous solution. The adsorption of tetracycline onto the magnetic mesoporous silica was a monolayer endothermic process. The maximum tetracycline adsorption capacity of magnetic mesoporous silica in aqueous solutions was 276.74 mg/g at 60 °C. With the adsorption, the pseudo-first-order model accurately reflects the data on adsorption kinetics, while the Langmuir model for adsorption matches the data on adsorption isotherms well. Tetracycline adsorption

by the MMS was spontaneous due to the negative values of the Gibbs free-energy and enthalpy change, and at the higher temperature the adsorption was adversely affected. The adsorbent showed exceptional properties, including tetracycline removal efficiency and easy separation from aqueous media by a magnet. Therefore, magnetic mesoporous silica could be used as a potential adsorbent for tetracycline from an aqueous solution. Furthermore, this adsorbent can be utilized as an environmentally friendly adsorbent for the treatment of wastewater.

Supplementary Materials: The following supporting information can be downloaded at: https://www.mdpi.com/article/10.3390/su15064727/s1, Table S1: Chemical compositions of Bottom Ash - Biomass Power Plant by XRF; Table S2: Chemical composition of SiO_2 extracted from Bottom Ash - Biomass Power Plant by XRF.

References

1. Cycoń, M.; Mrozik, A.; Piotrowska-Seget, Z. Antibiotics in the Soil Environment—Degradation and Their Impact on Microbial Activity and Diversity. *Front. Microbiol.* **2019**, *10*, 338. [CrossRef]
2. Chopra, I.; Roberts, M. Tetracycline Antibiotics: Mode of Action, Applications, Molecular Biology, and Epidemiology of Bacterial Resistance. *Microbiol. Mol. Biol. Rev.* **2001**, *65*, 232–260. [CrossRef]
3. Ötker, H.M.; Akmehmet-Balcıoğlu, I. Adsorption and degradation of enrofloxacin, a veterinary antibiotic on natural zeolite. *J. Hazard. Mater.* **2005**, *122*, 251–258. [CrossRef]
4. Kim, S.; Shon, H.; Ngo, H. Adsorption characteristics of antibiotics trimethoprim on powdered and granular activated carbon. *J. Ind. Eng. Chem.* **2010**, *16*, 344–349. [CrossRef]
5. Luo, Y.; Xu, L.; Rysz, M.; Wang, Y.; Zhang, H.; Alvarez, P.J.J. Occurrence and Transport of Tetracycline, Sulfonamide, Quinolone, and Macrolide Antibiotics in the Haihe River Basin, China. *Environ. Sci. Technol.* **2011**, *45*, 1827–1833. [CrossRef] [PubMed]
6. Yu, D.; Yi, X.; Ma, Y.; Yin, B.; Zhuo, H.; Li, J.; Huang, Y. Effects of administration mode of antibiotics on antibiotic resistance of Enterococcus faecalis in aquatic ecosystems. *Chemosphere* **2009**, *76*, 915–920. [CrossRef]
7. Javid, A.; Mesdaghinia, A.; Nasseri, S.; Mahvi, A.H.; Alimohammadi, M.; Gharibi, H. Assessment of tetracycline contamination in surface and groundwater resources proximal to animal farming houses in Tehran, Iran. *J. Environ. Health Sci. Eng.* **2016**, *14*, 1–5. [CrossRef] [PubMed]
8. Le, T.-H.; Ng, C.; Tran, N.H.; Chen, H.; Gin, K.Y.-H. Removal of antibiotic residues, antibiotic resistant bacteria and antibiotic resistance genes in municipal wastewater by membrane bioreactor systems. *Water Res.* **2018**, *145*, 498–508. [CrossRef] [PubMed]
9. Hamscher, G.; Sczesny, S.; Höper, H.; Nau, H. Determination of Persistent Tetracycline Residues in Soil Fertilized with Liquid Manure by High-Performance Liquid Chromatography with Electrospray Ionization Tandem Mass Spectrometry. *Anal. Chem.* **2002**, *74*, 1509–1518. [CrossRef] [PubMed]
10. Tolls, J. Sorption of Veterinary Pharmaceuticals in Soils: A Review. *Environ. Sci. Technol.* **2001**, *35*, 3397–3406. [CrossRef]
11. Zhang, Z.; Li, H.; Liu, H. Insight into the adsorption of tetracycline onto amino and amino–Fe^{3+} gunctionalized mesoporous silica: Effect of functionalized groups. *J. Environ. Sci.* **2018**, *65*, 171–178. [CrossRef]
12. Lv, J.-M.; Ma, Y.-L.; Chang, X.; Fan, S.-B. Removal and removing mechanism of tetracycline residue from aqueous solution by using Cu-13X. *Chem. Eng. J.* **2015**, *273*, 247–253. [CrossRef]

13. Ji, L.; Chen, W.; Duan, L.; Zhu, D. Mechanisms for strong adsorption of tetracycline to carbon nanotubes: A comparative study using activated carbon and graphite as adsorbents. *Environ. Sci. Technol.* **2009**, *43*, 2322–2327. [CrossRef] [PubMed]

14. Wang, H.; Yao, H.; Sun, P.; Pei, J.; Li, D.; Huang, C.-H. Oxidation of tetracycline antibiotics induced by Fe(III) ions without light irradiation. *Chemosphere* **2015**, *119*, 1255–1261. [CrossRef]

15. Zhao, C.; Deng, H.; Li, Y.; Liu, Z. Photodegradation of oxytetracycline in aqueous by 5A and 13X loaded with TiO$_2$ under UV irradiation. *J. Hazard. Mater.* **2010**, *176*, 884–892. [CrossRef] [PubMed]

16. Chang, B.; Hsu, F.; Liao, H. Biodegradation of three tetracyclines in swine wastewater. *J. Environ. Sci. Health Part B* **2014**, *49*, 449–455. [CrossRef]

17. Zazouli, M.A.; Susanto, H.; Nasseri, S.; Ulbricht, M. Influences of solution chemistry and polymeric natural organic matter on the removal of aquatic pharmaceutical residuals by nanofiltration. *Water Res.* **2009**, *43*, 3270–3280. [CrossRef]

18. Xiang, Y.; Xu, Z.; Wei, Y.; Zhou, Y.; Yang, X.; Yang, Y.; Yang, J.; Zhang, J.; Luo, L.; Zhou, Z. Carbon-based materials as adsorbent for antibiotics removal: Mechanisms and influencing factors. *J. Environ. Manag.* **2019**, *237*, 128–138. [CrossRef]

19. Hawker, D.W.; Chimpalee, D.; Vijuksangsith, P.; Boonsaner, M. The pH dependence of the cellulosic membrane permeation of tetracycline antibiotics. *J. Environ. Chem. Eng.* **2015**, *3*, 2408–2415. [CrossRef]

20. Ahmed, M.J. Adsorption of quinolone, tetracycline, and penicillin antibiotics from aqueous solution using activated carbons: Review. *Environ. Toxicol. Pharmacol.* **2017**, *50*, 1–10. [CrossRef]

21. Putra, E.K.; Pranowo, R.; Sunarso, J.; Indraswati, N.; Ismadji, S. Performance of activated carbon and bentonite for adsorption of amoxicillin from wastewater: Mechanisms, isotherms and kinetics. *Water Res.* **2009**, *43*, 2419–2430. [CrossRef] [PubMed]

22. Gao, Y.; Li, Y.; Zhang, L.; Huang, H.; Hu, J.; Shah, S.M.; Su, X. Adsorption and removal of tetracycline antibiotics from aqueous solution by graphene oxide. *J. Colloid Interface Sci.* **2012**, *368*, 540–546. [CrossRef] [PubMed]

23. Choi, K.-J.; Kim, S.-G.; Kim, S.-H. Removal of antibiotics by coagulation and granular activated carbon filtration. *J. Hazard. Mater.* **2008**, *151*, 38–43. [CrossRef]

24. Li, Z.; Schulz, L.; Ackley, C.; Fenske, N. Adsorption of tetracycline on kaolinite with pH-dependent surface charges. *J. Colloid Interface Sci.* **2010**, *351*, 254–260. [CrossRef]

25. Yu, F.; Li, Y.; Han, S.; Ma, J. Adsorptive removal of antibiotics from aqueous solution using carbon materials. *Chemosphere* **2016**, *153*, 365–385. [CrossRef] [PubMed]

26. Mesa, M.; Sierra, L.; Patarin, J.; Guth, J.-L. Morphology and porosity characteristics control of SBA-16 mesoporous silica. Effect of the triblock surfactant Pluronic F127 degradation during the synthesis. *Solid State Sci.* **2005**, *7*, 990–997. [CrossRef]

27. Anbia, M.; Lashgari, M. Synthesis of amino-modified ordered mesoporous silica as a new nano sorbent for the removal of chlorophenols from aqueous media. *Chem. Eng. J.* **2009**, *150*, 555–560. [CrossRef]

28. Kresge, C.T.; Leonowicz, M.E.; Roth, W.J.; Vartuli, J.C.; Beck, J.S. Ordered Mesoporous Molecular Sieves Synthesized by a Liquid-Crystal Template Mechanism. *Nature* **1992**, *359*, 710–713. [CrossRef]

29. Wu, S.H.; Lin, H.P. Synthesis of mesoporous silica nanoparticles. *Chem. Soc. Rev.* **2013**, *42*, 3862–3875. [CrossRef]

30. Diagboya, P.N.; Olu-Owolabi, B.I.; Adebowale, K.O. Microscale scavenging of pentachlorophenol in water using amine and tripolyphosphate-grafted SBA-15 silica: Batch and modeling studies. *J. Environ. Manag.* **2014**, *146*, 42–49. [CrossRef]

31. Sathe, T.R.; Agrawal, A.; Nie, S. Mesoporous Silica Beads Embedded with Semiconductor Quantum Dots and Iron Oxide Nanocrystals: Dual-Function Microcarriers for Optical Encoding and Magnetic Separation. *Anal. Chem.* **2006**, *78*, 5627–5632. [CrossRef] [PubMed]

32. Zuo, B.; Li, W.; Wu, X.; Wang, S.; Deng, Q.; Huang, M. Recent Advances in the Synthesis, Surface Modifications and Applications of Core-Shell Magnetic Mesoporous Silica Nanospheres. *Chem. Asian J.* **2020**, *15*, 1248–1265. [CrossRef] [PubMed]

33. Diagboya, P.N.; Dikio, E.D. Silica-based mesoporous materials; emerging designer adsorbents for aqueous pollutants removal and water treatment. *Microporous Mesoporous Mater.* **2018**, *266*, 252–267. [CrossRef]

34. Yue, Q.; Zhang, Y.; Wang, C.; Wang, X.; Sun, Z.; Hou, X.-F.; Zhao, D.; Deng, Y. Magnetic yolk–shell mesoporous silica microspheres with supported Au nanoparticles as recyclable high-performance nanocatalysts. *J. Mater. Chem. A* **2015**, *3*, 4586–4594. [CrossRef]

35. Faaliyan, K.; Abdoos, H.; Borhani, E.; Afghahi, S.S.S. Magnetite-silica nanoparticles with core-shell structure: Single-step synthesis, characterization and magnetic behavior. *J. Sol-Gel Sci. Technol.* **2018**, *88*, 609–617. [CrossRef]

36. Cho, B.H.; Nam, B.H.; An, J.; Youn, H. Municipal Solid Waste Incineration (MSWI) Ashes as Construction Materials—A Review. *Materials* **2020**, *13*, 3143. [CrossRef]

37. Zhai, J.; Burke, I.T.; Stewart, D.I. Beneficial management of biomass combustion ashes. *Renew. Sustain. Energy Rev.* **2021**, *151*, 111555. [CrossRef]

38. Yang, G.C.; Yang, T.-Y. Synthesis of zeolites from municipal incinerator fly ash. *J. Hazard. Mater.* **1998**, *62*, 75–89. [CrossRef]

39. Fan, Y.; Zhang, F.-S.; Zhu, J.; Liu, Z. Effective utilization of waste ash from MSW and coal co-combustion power plant—Zeolite synthesis. *J. Hazard. Mater.* **2008**, *153*, 382–388. [CrossRef]

40. Chandrasekar, G.; You, K.-S.; Ahn, J.-W.; Ahn, W.-S. Synthesis of hexagonal and cubic mesoporous silica using power plant bottom ash. *Microporous Mesoporous Mater.* **2008**, *111*, 455–462. [CrossRef]

41. Chen, D.; Zhang, Y.; Xu, Y.; Nie, Q.; Yang, Z.; Sheng, W.; Qian, G. Municipal solid waste incineration residues recycled for typical construction materials—A review. *RSC Adv.* **2022**, *12*, 6279–6291. [CrossRef] [PubMed]

42. Liu, Z.-S.; Li, W.-K.; Huang, C.-Y. Synthesis of mesoporous silica materials from municipal solid waste incinerator bottom ash. *Waste Manag.* **2014**, *34*, 893–900. [CrossRef] [PubMed]

43. Li, Y.; Wang, R.; Chen, Z.; Zhao, X.; Luo, X.; Wang, L.; Li, Y.; Teng, F. Preparation of magnetic mesoporous silica from rice husk for aflatoxin B1 removal: Optimum process and adsorption mechanism. *PLoS ONE* **2020**, *15*, e0238837. [CrossRef]

44. Jabariyan, S.; Zanjanchi, M.A. A simple and fast sonication procedure to remove surfactant templates from mesoporous MCM-41. *Ultrason. Sonochemistry* **2012**, *19*, 1087–1093. [CrossRef] [PubMed]

45. Ahangaran, F.; Hassanzadeh, A.; Nouri, S. Surface modification of Fe3O4@SiO2 microsphere by silane coupling agent. *Int. Nano Lett.* **2013**, *3*, 23. [CrossRef]

46. Gu, C.; Karthikeyan, K.G. Interaction of Tetracycline with Aluminum and Iron Hydrous Oxides. *Environ. Sci. Technol.* **2005**, *39*, 2660–2667. [CrossRef]

47. Prakasham, R.S.; Devi, G.S.; Laxmi, K.R.; Rao, C.S. Novel Synthesis of Ferric Impregnated Silica Nanoparticles and Their Evaluation as a Matrix for Enzyme Immobilization. *J. Phys. Chem. C* **2007**, *111*, 3842–3847. [CrossRef]

48. Zhang, Z.; Lan, H.; Liu, H.; Li, H.; Qu, J. Iron-incorporated mesoporous silica for enhanced adsorption of tetracycline in aqueous solution. *RSC Adv.* **2015**, *5*, 42407–42413. [CrossRef]

49. Suwunwong, T.; Patho, P.; Choto, P.; Phoungthong, K. Enhancement the rhodamine 6G adsorption property on Fe3O4-composited biochar derived from rice husk. *Mater. Res. Express* **2020**, *7*. [CrossRef]

50. Wang, J.; Guo, X. Adsorption isotherm models: Classification, physical meaning, application and solving method. *Chemosphere* **2020**, *258*, 127279. [CrossRef]

51. Bruckmann, F.D.S.; Schnorr, C.E.; Salles, T.d.R.; Nunes, F.B.; Baumann, L.; Müller, E.I.; Silva, L.F.O.; Dotto, G.L.; Rhoden, C.R.B. Highly Efficient Adsorption of Tetracycline Using Chitosan-Based Magnetic Adsorbent. *Polymers* **2022**, *14*, 4854. [CrossRef] [PubMed]

52. Jiang, Z.; Hu, D. Molecular mechanism of anionic dyes adsorption on cationized rice husk cellulose from agricultural wastes. *J. Mol. Liq.* **2018**, *276*, 105–114. [CrossRef]

53. Liu, Y. Is the Free Energy Change of Adsorption Correctly Calculated? *J. Chem. Eng. Data* **2009**, *54*, 1981–1985. [CrossRef]

54. Dai, J.; Meng, X.; Zhang, Y.; Huang, Y. Effects of modification and magnetization of rice straw derived biochar on adsorption of tetracycline from water. *Bioresour. Technol.* **2020**, *311*, 123455. [CrossRef]

55. Jang, H.M.; Kan, E. A novel hay-derived biochar for removal of tetracyclines in water. *Bioresour. Technol.* **2018**, *274*, 162–172. [CrossRef]

56. Jang, H.M.; Yoo, S.; Choi, Y.-K.; Park, S.; Kan, E. Adsorption isotherm, kinetic modeling and mechanism of tetracycline on Pinus taeda-derived activated biochar. *Bioresour. Technol.* **2018**, *259*, 24–31. [CrossRef]

57. Li, H.; Hu, J.; Meng, Y.; Su, J.; Wang, X. An investigation into the rapid removal of tetracycline using multilayered graphene-phase biochar derived from waste chicken feather. *Sci. Total. Environ.* **2017**, *603–604*, 39–48. [CrossRef] [PubMed]

58. Premarathna, K.; Rajapaksha, A.U.; Adassoriya, N.; Sarkar, B.; Sirimuthu, N.M.; Cooray, A.; Ok, Y.S.; Vithanage, M. Clay-biochar composites for sorptive removal of tetracycline antibiotic in aqueous media. *J. Environ. Manag.* **2019**, *238*, 315–322. [CrossRef]

59. Nguyen, V.-T.; Nguyen, T.-B.; Chen, C.-W.; Hung, C.-M.; Vo, T.-D.-H.; Chang, J.-H.; Dong, C.-D. Influence of pyrolysis temperature on polycyclic aromatic hydrocarbons production and tetracycline adsorption behavior of biochar derived from spent coffee ground. *Bioresour. Technol.* **2019**, *284*, 197–203. [CrossRef]

60. Yu, C.; Chen, X.; Li, N.; Chen, J.; Yao, L.; Zhou, Y.; Lu, K.; Lai, Y.; Lai, X. Biomass ash pyrolyzed from municipal sludge and its adsorption performance toward tetracycline: Effect of pyrolysis temperature and KOH activation. *Environ. Sci. Pollut. Res.* **2022**, *29*, 81383–81395. [CrossRef]

61. Chang, J.; Shen, Z.; Hu, X.; Schulman, E.; Cui, C.; Guo, Q.; Tian, H. Adsorption of Tetracycline by Shrimp Shell Waste from Aqueous Solutions: Adsorption Isotherm, Kinetics Modeling, and Mechanism. *ACS Omega* **2020**, *5*, 3467–3477. [CrossRef] [PubMed]

VITAE

Name   Phan Thi Hong Hanh

Student ID   6410920043

Educational Attainment

Degree	Name of Institution	Year of Graduation
B.Eng Environmental Engineering	Nong Lam University, Ho Chi Minh City, Vietnam	2017

Scholarship Awards during Enrolment

Faculty Grant and Graduate School Grant.

Graduate Research Development Grant.

Work – Position and Address

....

List of Publication and Proceeding

1. Hanh, P.T.H.; Phoungthong, K.; Chantrapromma, S.; Choto, P.; Thanomsilp, C.; Siriwat, P.; Wisittipanit, N.; Suwunwong, T.Adsorption of Tetracycline by Magnetic Mesoporous Silica Derived from Bottom Ash—Biomass Power Plant. *Sustainability* 2023, *15*, 4727. https://doi.org/10.3390/su15064727.